



## Stress corrosion cracking behaviour of 7xxx aluminum alloys: A literature review

A. C. UMAMAHESHWER RAO<sup>1</sup>, V. VASU<sup>1</sup>, M. GOVINDARAJU<sup>2</sup>, K. V. SAI SRINADH<sup>1</sup>

1. Department of Mechanical Engineering, National Institute of Technology Warangal, Warangal 506004, India;

2. Nonferrous Materials Technology Development Centre, Hyderabad-500 058, 500005, India

Received 15 July 2015; accepted 11 March 2016

**Abstract:** Stress corrosion cracking (SCC) is degradation of mechanical properties under the combined action of stress and corrosive environment of the susceptible material. Out of eight series of aluminium alloys, 2xxx, 5xxx and 7xxx aluminium alloys are susceptible to SCC. Among them, 7xxx series aluminium alloys have specific application in aerospace, military and structural industries due to superior mechanical properties. In these high strength 7xxx aluminium alloys, SCC plays a vital factor of consideration, as these failures are catastrophic during the service. The understanding of SCC behaviour possesses critical challenge for this alloy. The main aim of this review paper is to understand the effect of constituent alloying elements on the response of microstructural variation in various heat-treated conditions on SCC behavior. Further, review was made for improving the SCC resistance using thermomechanical treatments and by surface modifications of 7xxx alloys. Apart from a brief review on SCC of 7xxx alloys, this paper presents the effect of stress and pre-strain, effect of constituent alloying elements in the alloy, and the effect of environments on SCC behaviour. In addition, the SCC behaviours of weldments, 7xxx metal matrix composites and also laser surface modifications were also reviewed.

**Key words:** 7xxx aluminum alloy; stress corrosion cracking; heat treatment; microstructure; corrosive environment; thermo-mechanical treatment

### 1 Stress corrosion cracking

Stress corrosion cracking (SCC) is degradation or crack process that occurs in susceptible alloys such as in certain Al alloys and in steels, and occurs when three situation must simultaneously present, namely, the elements of the material alloy must be susceptible to SCC, the tensile stresses should be higher than some threshold value and a particular crack-promoting surroundings environment. This failure occurs in potentially susceptible structural alloys and under service conditions, which can fail often without any prior warning, and lead to catastrophic failure.

The main factor which has vital effect on the SCC behavior is the alloy composition. The composition of the material affects the formation and stability of a protecting film on the surface of the alloy. Also, these alloying elements may influence the strength, grain boundaries, grain size and orientation, grain-boundary segregation, and residual stresses within the material.

SCC takes place in aggressive environment such as in  $\text{Cl}^-$ ,  $\text{Br}^-$  and  $\text{I}^-$  aqueous solutions and also in moist air and distill water. The environmental parameters must be in specific ranges for cracking to occur. The environmental parameters are temperature, pH, electrochemical potential, solute species, solute concentration and oxygen concentration. To activate SCC, a critical threshold stress must be present. This critical threshold stress may be considered as internal stress or residual stress or external stress. The SCC process consists of two different phenomena which are crack initiation and crack propagation. The cracking rate is strongly reliant on the applied stress intensity throughout the crack propagation stage, and can be further divided into three different stages, as illustrated in Fig. 1.

During the crack initiation stage in the material, stress intensity or mechanical stress and corrosion environment interact with each other until the local conditions in the crack tip region reach a critical state that promotes the propagation of cracks. This stage is

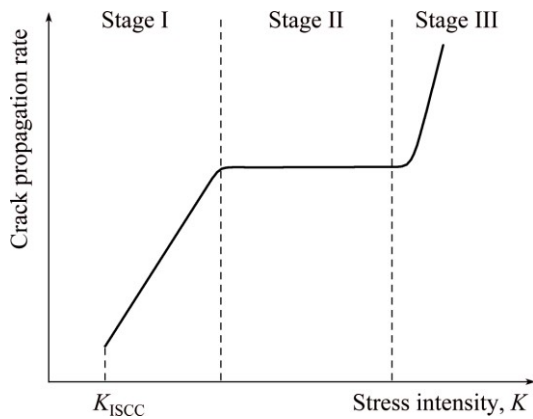


**Fig. 1** Three stages of stress corrosion crack propagation

usually known as “incubation period” and related with a period of time with no apparent crack growth [1]. Usually, surface discontinuities and corrosion pits are the main causes for the SCC initiation which are illustrated in Fig. 2 [2].

SCC initiated from surface discontinuities such as laps, grooves, burrs and cracking of inclusions resulted from machining or fabrication process, as well as pre-existing cracks and grain boundaries that have significantly different electrochemical properties with the bulk material.

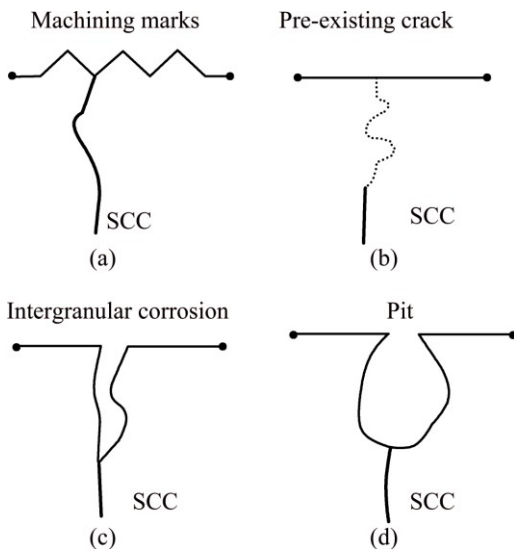


**Fig. 2** Types of crack initiation sites of SCC: (a) Machining marks; (b) Pre-existing crack; (c) Intergranular corrosion; (d) Pit

SCC can also initiate from pits formed due to corrosion, where the local environment within the pits can be much harsher compared with the bulk environment, reducing the protective effect of oxide films and promoting the transition from crack initiation to crack propagation. This type of crack initiation was further discussed by many other researchers [3,4].

When the stress corrosion crack starts to propagate,

the cracking rate becomes dependent on the applied stress intensity. However, based on strong changes in the stress intensity dependence, the cracking rate vs stress intensity graph consists of three distinct stages, Stages I, II, and III, respectively. As shown in Fig. 1, in Stage I, when the stress intensity is higher than the threshold value  $K_{ISCC}$ , the crack propagation rate has large stress intensity dependence and can be approximated by an exponential function, i.e., a straight line in a logarithmic–linear plot. The crack propagation enters Stage II at higher stress intensity levels. In this stage, the crack rate is freelance of the applied stress intensity and is usually represented as a “plateau”. There are many other factors that can affect this “plateau” crack propagation rate, such as loading mode (Mode I or Mode III), chemistry of the corrosive solution, electrochemical potential, and relative humidity [5]. When the stress intensity becomes even higher, the crack propagation rate becomes stress intensity dependent again. However, cracking at this stage is more related to mechanical fracture rather than SCC.

A biaxial or triaxial stress is created in the region of the stress raiser such as crack. The stress concentration at the crack tip produces high localized stresses that surpass the yield strength of the metal in the section neighboring the crack tip. This region is referred to as the plastic zone. The size of the plastic zone depends on applied stress intensity and yield strength of the material. Under plane strain conditions, the size or radius is estimated by the following equation:

$$r_y \approx (1/6\pi)(K^2/\sigma_{ys}^2) \quad (1)$$

The high triaxial stresses in this plastic zone prior the crack tip give potential sites for buildup of hydrogen that enters the metal by diffusion from the surface [6]. It was determined that hydrogen would be attracted to the triaxial stress region attributable to the dilational field. Inflection of a stress generates chemical potential gradient driving hydrogen to the triaxial stress region and diffusion happens as per the Einstein drift equation:

$$J = -(Dc/kT)(\delta\mu/\delta R) \quad (2)$$

High hydrogen fugacities on the order of  $10^{40}$  atmospheres are possible in the triaxial stress region [7].

They are many SCC mechanisms which ultimately lead to failure. Till now the reported SCC mechanisms are hydrogen enhanced localized plasticity (HELP), film induced cleavage, hydride formation, slip dissolution, hydrogen enhanced decohesion (HEDE), corrosion enhanced localized plasticity (CELP) and adsorption induced dislocation emission (AIDE). The specific mechanism that is operative depends on the type of material, environment, and loading conditions. Most of the researchers reported that SCC mechanisms in high

strength Al-alloys are hydrogen induced cracking [8,9] anodic dissolution assisted cracking and passive film rupture as shown in Fig. 3 [5,10,11].

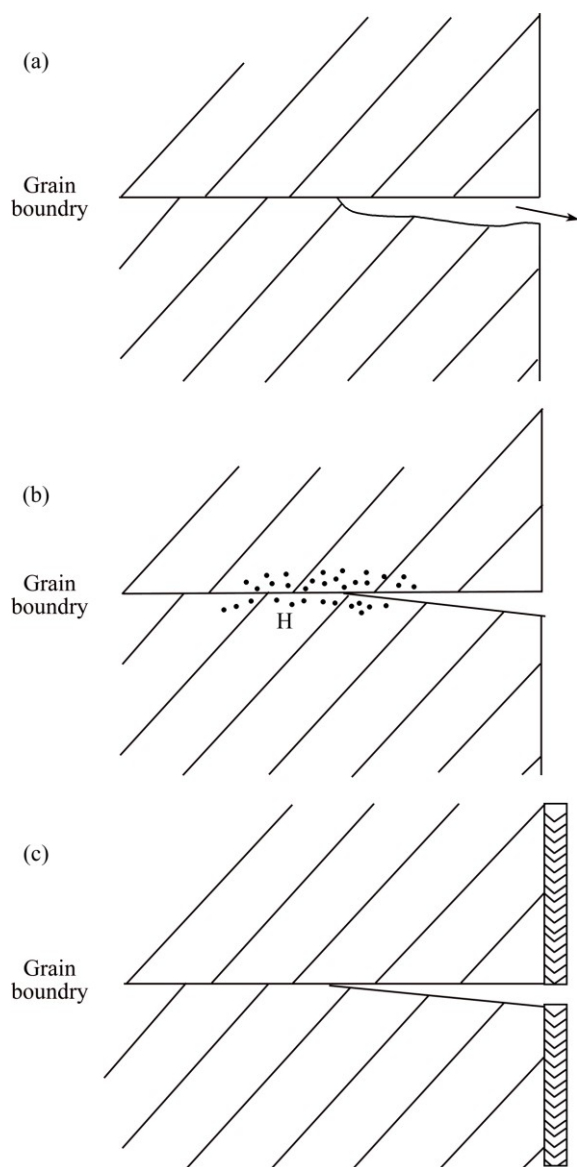


**Fig. 3** Illustration of mechanisms of SCC for aluminum alloys [10]

**Hydrogen induced cracking:** The small size hydrogen ion can pass into the lattice sites of the material alloy in both gaseous phases and aqueous phases.

In an aqueous phase where corrosion reactions take place, both anodic and corresponding cathodic reactions occur. In many cases, hydrogen ion reduction is the cathodic reaction where hydrogen atoms are formed on the surface. On the other hand, hydrogen atoms combine to form hydrogen gas, other hydrogen atoms remain adsorbed to the surface. Because of the high partial hydrogen pressure, there exists a driving force for the hydrogen atoms to be absorbed into the lattice causing embrittling the lattices leading to intergranular failure.

Al–Zn–Mg–Cu–Zr alloy underwent hydrogen embrittlement even in laboratory air (having a relative humidity of ~50%), this was observed by BOBBY-KANNAN et al [11] and Speidel has shown that the increase in relative humidity enhanced the SCC crack velocity significantly in 7075 Al alloy. The effect of hydrogen embrittlement will be diminished by providing hydrogen sites like lattice defects such as dislocations, vacancies, grain boundaries and precipitates offer a range of trappings sites for hydrogen diffusion. One of the best heat treatments for 7xxx alloys is overaging which provides efficient tapping sites for hydrogen inhibition into the lattice sites. This heat treatment provides coarser precipitates along the grain boundaries with some interparticle acting as trapping sites for hydrogen ions.

**Anodic dissolution assisted cracking:** Anodic dissolution assisted cracking is characteristically an intergranular mode of failure. Anodic dissolution will proceed when the grain boundaries or grain adjacent regions should be anodic to the rest of the microstructure, so that the dissolution proceeds selectively along the boundaries. It has been reported by many authors that, in the alloys such as Al–Zn–Mg–Cu–Zr and 7039 that the passive film breakdown in the vicinity of copper rich intermetallic caused the crack initiation in the alloy. Fracture surface analysis in their studies reported that the continuous nature of anodic grain boundary precipitates caused easy dissolution, leading to crack propagation and underwent intergranular stress corrosion cracking.

Aluminum alloys have excellent formability, high specific strength and good machinability. Due to this reason, these alloys are used in aircraft structures, automobile components and in structural components. Aluminum and its alloys are resistant to corrosion as they have  $\text{Al}_2\text{O}_3$  layer formed on the surface. The high strength Al alloys are prone to SCC due to presence of constituent alloying elements. Among the eight series of Al alloys, SCC is most common in 2xxx, 5xxx and 7xxx (alloys containing Mg) series Al alloys. Precipitation-hardening alloys containing soluble alloying elements, such as Mg, Cu, Si and Zn are susceptible to SCC. It was reported that more aircraft components made of 7079-T6, 7075-T6 and 2024-T3 Al-alloys failed in the year from 1960 to 1970 and these failures were attributed to the SCC [5].

In 2xxx series alloys, the major constituents are copper and magnesium and the strength of the alloy is attained in this alloy due to the formation of the precipitation hardening of the constituent alloying elements which is achieved by solution heat treatment followed by rapid cooling either by artificial aging at elevated temperature T6 or by natural aging.

SCC has major influences in the 2xxx series alloys as the main constituents of the alloy are Cu and Mg

which have an alarming effect on the EAC. SCC behavior in 2xxx series depends on the composition and the heat treatment followed. It has been reported that this series alloys, such as 2024, 2014, and 2219 in the T3 and T4 tempers are more susceptible to SCC in the short transverse direction [12,13].

Also, it has been reported that SCC resistance is further decreased if these alloys are in the T3 and T4 tempers conditions and heated for short periods in the temperature range used for artificial aging. It has been observed that SCC resistance declination can be caused due to the formation of exclusive precipitation (coarsened Al–Cu) along the grain boundary which depletes the regions adjacent to the grain boundaries of solute. In the formed precipitates, Cu is the major element which makes the material very prone to intergranular pitting, corrosion and SCC. This copper-rich precipitates zone along the grain boundary is more noble/cathodic which creates the potential difference between the aluminum matrix, hence acts as a galvanic coupling between matrix and the formed precipitates result in localized corrosion. The resistance to SCC of these alloys can be enhanced by heating for longer time, as specified for the T6 and T8 tempers, the precipitation becomes more homogeneous.

Apart from 2xxx Al alloys, Al–Li alloys (such as 2090 and 8090) are more susceptible to intergranular SCC. These Al–Li alloys have higher strength as compared to rest of 2xxx alloys [14,15]. In the peak aged condition, these alloys have high SCC resistance and moderate resistance in overaging condition. But, in underaged condition, these alloys are more prone to SCC.

The formation of intermetallic precipitates such as  $\text{Al}_2\text{CuLi}$  at the grain boundaries increases SCC susceptibility of the underaged alloys of the Al–Li alloys. These formed  $\text{Al}_2\text{CuLi}$  precipitates are observed to be more anodic to the copper-rich matrix, leading to crack tip anodic dissolution along the grain boundaries.

It has been reported that with increasing aging time, copper-containing precipitates form inside the grains. It has been hypothesized that the formation of these precipitates may increase the anode-cathode area ratio in the microstructure such that preferential grain boundary attack is avoided. Similar behavior has been observed with SCC of Al–Li–Cu–Mg alloys such as 8090 [16].

5xxx series Al alloys are more susceptible to SCC when cold-rolled and at stabilizing tempers with magnesium contents above 5%. In this alloy, it owns highly supersaturated of solid solution, which tends to expel the excess magnesium precipitate such as  $\text{Mg}_2\text{Al}_3$  along the grain boundary without forming in the grains, which is more anodic to the alloy matrix, and this results in SCC susceptibility [17].

Counterparts on the 5xxx series Al alloys containing low Mg show no intergranular SCC as they do not form any precipitates at the grain boundaries. While alloys exceeding magnesium concentrations of approximately 3%, such as 5083, when in strain-hardened tempers, may develop susceptible microstructures as a result of heating or even after long time at room temperature. It was observed that the anodic dissolution and diffusion of the hydrogen mechanisms lead to SCC in 5xxx series alloys.

While 6xxx Al alloys are very less prone to SCC. Till date there have been no reported cases of SCC of this group of alloys, certain abnormal thermal treatments, such as a high solution annealing temperature, followed by a slow quenching, can make these alloys susceptible to SCC in the naturally aged T4 condition.

Previously, it was stated that among the eight series of aluminum alloys, 2xxx, 5xxx, and 7xxx alloys are susceptible to SCC. As compared to 2xxx and 5xxx Al alloys, 7xxx alloys have specific structural and aerospace applications due to superior mechanical properties. The major application of 7xxx is in the field of aerospace industry, military, nuclear and also in the structural parts of building application because of high strength, ductility, toughness, low density and good fatigue properties. But, SCC resistance is of greater importance in this alloy, since many failures of aircraft structures and components have occurred by SCC since the 1950's [18].

The main components of the 7xxx Al alloy are Zn, Mg, Cu and minor Fe and trace of other intermetallic elements such as Zr, Cr, Si and Mn. In general, Al–Zn–Mg–Cu alloys have high potential to recrystallize easily during deformation and subsequent heat treatments ultimately form recrystallized grain boundary with addition of high angle grain boundary could preferentially erode and crack, which is objectionable for applications. Alloying elements such as Mn, Cr or Zr are commonly added to enhance the recrystallization resistance of Al–Zn–Mg–Cu alloys. On the other hand, the recrystallization of Al–Zn–Mg–Cu alloy cannot be completely suppressed by Mn, Cr or Zr addition although addition of Zr is proven more effective and widely used [19]. Aluminium 7050 and 7075 are both majorly used for airframe structures. Both alloys have common constituent alloying elements, except Cr is replaced by Zr in case of 7050 alloys. In addition, 7050 Al alloy containing minor Si and Fe contents than 7075 improves the fracture toughness and it has high Cu content than 7075 which enhances the strength and SCC resistance by increasing the temperature range of GP zone stability. 7050 Al alloy is superior than 7075 alloy in overall aspects, for example, it has a good combination of strength, toughness and SCC resistance. The better properties of 7050 are attributed to the presence of Zr, which is responsible for the

microstructure stability. The addition of Zr stabilizes the GP zone in a wider range of temperatures therefore, the mechanical properties and SCC resistance are reported to be high. It has been reported that 7050 Al alloy is highly quenching sensitive and hard to fabricate thicker sections of consistent strength. It is found that by replacing Zr with Cr, quenching sensitivity can be substantially reduced and desired recrystallisation suppressing effect of Cr is maintained [20–22]. The SCC phenomenon is very complex to understand and it depends on several factors. On the initiation of crack, its growth is influenced by combination of factors such as microstructure of the material which includes heat treatment, the amount of impurities, manufacturing background, etc., and the aggressive conditions in the environment and finally the level of stresses. In this review, factors affecting stress corrosion cracking of 7xxx series, mainly on 7075 and 7050 Al alloys are reviewed as they have wider applications among the 7xxx series alloys in field of aerospace and structural industries.

## 2 Factors affecting stress corrosion cracking (SCC)

### 2.1 Effect of composition on SCC

The composition of the material has a vital role in mechanical properties and in SCC behavior. Segregation and precipitation of alloying elements along the grain boundaries play a critical role in the SCC and on tensile behavior. 7xxx series alloys comprise two types of constituent particles contributing to high strength and SCC: 1) Precipitates like Al, Mg and Zn are anodic to the matrix and readily dissolve; 2) Precipitates such as Fe, Cu and Mn are cathodic to the matrix and tend to boost dissolution of the adjacent matrix. Zn and Mg combine to form  $MgZn_2$  precipitate known as  $\eta$  phase. The strength of the alloy is improved by the presence of fine  $MgZn_2$  precipitates in the grains, this phase acts as anode to the matrix phase and hence in certain temper conditions, the precipitates are continuously developed along the grain boundary. The dissolution of these precipitates causes easy crack propagation under tensile stress, giving rise to SCC. In 7xxx alloys, observations of environmentally assisted cracking (EAC) are predominantly intergranular, hence, the enrichment or depletion of Mg, Zn, or Cu plays a key role in EAC resistance [23].

Many authors reported that there are two main mechanisms for SCC to occur in 7xxx series Al alloys which are reported to be hydrogen embrittlement and anodic dissolution. It was reported that the lattice diffusion coefficients of hydrogen ions are very low in FCC materials such as in this alloys, unfortunately, it is

observed that tendency of hydrogen transportation in this alloy was due to favorable conditions provided by the grain boundaries for the rapid diffusion of hydrogen. It has been reported that the SCC sensitivity of 7xxx alloys raises with the raise in Zn and Mg contents. Also, the SCC susceptibility depends on the ratio of these elements (Zn:Mg) [24,25]. On the other hand, Cu additions are known to improve the EIC performance of Al–Zn–Mg alloys. While the Zn, Mg and Cu alloy composition parameters are by far the most influential on SCC susceptibility, other alloy additions and impurities can have secondary influences on SCC behavior. GRUHL [24,25] conducted a series of experiments on Al–Zn–Mg–(Cu) alloys with a variety of compositions and thermal treatments and consequently observed a wide range of SCC susceptibility. He also used TEM and EDX to measure the Zn, Mg and Cu concentrations in solid solution in the grain boundary area. The most significant result was that there was a definite linear relationship between the concentration of Zn in solid solution and the logarithm of the time to failure at a constant stress level (Fig. 4). There was no apparent relation between Mg concentration in solid solution and SCC performance.

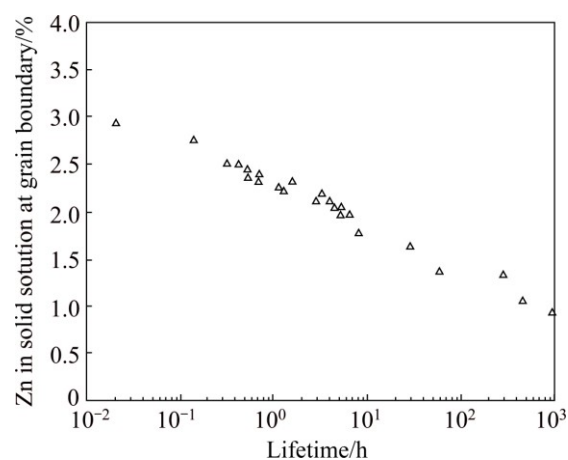


**Fig. 4** Relationship between Zn content of grain boundary area and time to fracture of Al–Zn–Mg–(Cu) alloys,  $\sigma=250$  MPa [25]

Gruhl's experiments on Al–Zn–Mg alloys with total solute content of (Zn+Mg) of 8% indicated that EIC resistance was optimized by maintaining a Zn:Mg ratio of 2.7 to 2.9 as illustrated in Fig. 5 [24,25]. This is an Zn:Mg mole ratio of  $\sim 1$ , which corresponds to the equilibrium line between the  $\alpha$ -phase and  $T$ -phase in the Al–Zn–Mg phase diagram. Addition of Cu improved the EIC resistance of Al–Zn–Mg alloys. In the peak-aged (T6) temper, addition of 1% Cu to the alloys with varying Zn:Mg ratios increases the “duration of life” or EIC resistance by an order of magnitude. Alloy development activities at Alcoa Technical Center have



also indicated similar influences of the Zn:Mg ratio and the Cu content on SCC resistance. However, the optimal Zn:Mg ratio appeared to vary somewhat with variations in the total solute. For experimental alloys with (Zn+Mg) contents of 4.5–6.0, the optimum Zn:Mg ratio was ~2.5 while for (Zn+Mg) contents somewhat greater than 8%, the optimum Zn:Mg ratio appeared to be greater than 3. SPEIDEL and HYATT [26] measured crack growth rates on AA7079 (4.3% Zn, 2.25% Mg, 0.6% Cu), AA7075 (5.6% Zn, 2.5% Mg, 1.6% Cu) and AA7178 (6.8% Zn, 2.75% Mg, 2.0% Cu) in saturated aqueous NaCl as a function of over-aging time. The crack growth rates for the peak-aged temper (no overaging in Fig. 6) of the higher Cu alloys are 2.5 to 3 orders of magnitude lower than that for the low Cu AA7079. The results also indicate a significant influence of Cu on the effectiveness of over-aging treatments for improving EIC resistance.

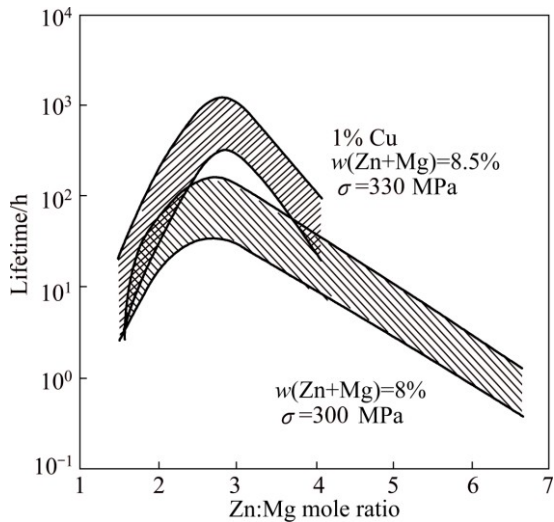


Fig. 5 Influence on Zn:Mg mole ratio on SCC susceptibility of Al-Zn-Mg and Al-Zn-Mg-Cu alloys

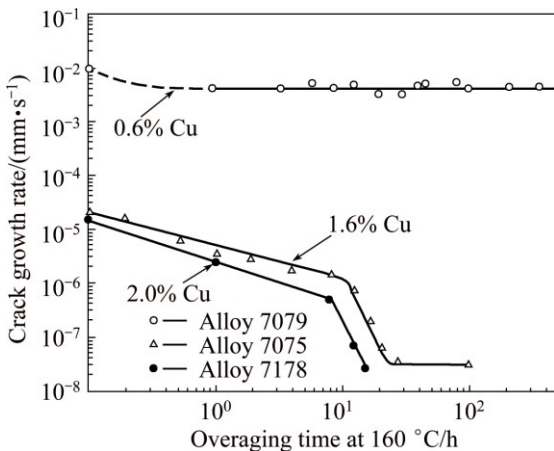


Fig. 6 Crack growth rates for 7xxx alloys with varying Cu contents as function of overaging time [5]

Over aging of the higher Cu alloys (7075 and 7178) significantly decreased crack growth rates, but over

aging of the low Cu alloy, 7079, did not substantially decrease the crack growth rate. It is also interesting to note that there appears a distinct change in the slope of the curve after ~10 h over aging at 160 °C for the high Cu alloys, implying that there may be two different rates controlling processes involved. The differences in EIC behavior for these three commercial alloys have been attributed to differences in Cu content, but it should also be noted that the Zn and Mg levels in these three alloys are different which could also affect the crack growth rates. Although all three alloys have Zn:Mg ratios less than the optimum 2.7–3.0 range, the low Cu AA7079 (Zn:Mg ratio of 1.9) also has a lower Zn:Mg ratio than the higher Cu alloys, AA7075 (Zn:Mg ratio of 2.2) and AA7178 (Zn:Mg ratio of 2.5) which could also contribute to differences in EIC susceptibility as previously discussed.

SARKAR et al [27] and BIRNBAUM [28] systematically evaluated the effect of Cu content and heat treatment on the stress corrosion characteristics of Al-6Zn-2Mg-xCu (i.e., 7050 type) alloy. The compositions, processing, and heat treatments were carefully controlled to obtain similar grain structures for all four Cu content variations so that the effects of Cu could be unambiguously evaluated. Their results indicated that Stage II crack growth rates of T651 temper decrease systematically as Cu content increases from 0 to 2.1% (Fig. 7). Over aging significantly decreased crack growth rates, even for the 0% Cu alloy (Fig. 8), but only after considerable over aging at a severe strength penalty.

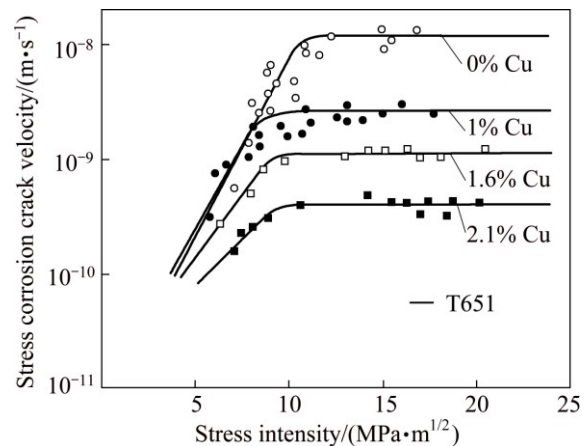
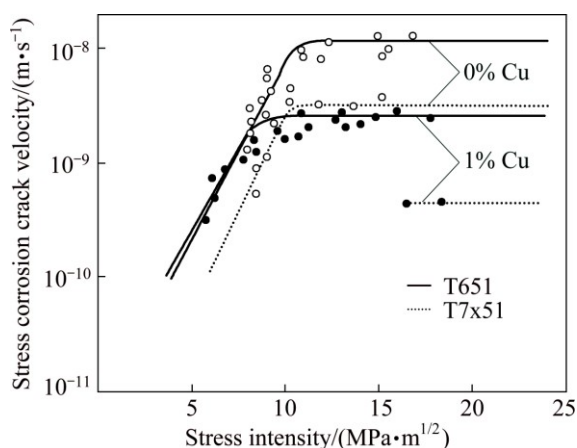


Fig. 7 Effect of stress intensity on stress corrosion crack velocity of Al-6Zn-2Mg-xCu in 3.5% NaCl for varying copper contents [27]

SONG et al [29] reported that the presence of Mg along the grain boundaries has larger electronegativity difference between Mg and H atoms than that between Al and H atoms. Consequently, the Mg and phases bearing Mg along the grain boundary have affinity to absorb hydrogen from the test solution and thus

accelerate its diffusion and increase the solution degree of hydrogen in the grain boundaries. This results in the grain boundary embrittlement and accelerates the propagation of the stress corrosion cracking. In contrast to this effect, larger inter-particle spacing of the grain boundary particles at the surface could decline anodic dissolution acceleration and act as the entrapping sites for atomic hydrogen further creates molecular hydrogen bubbles to decrease the concentration of the atomic hydrogen in the grain boundaries.



**Fig. 8** Effect of stress intensity on stress corrosion crack velocity of Al-6Zn-2Mg-xCu in 3.5% NaCl for T651 and T7x51 type aging treatments [27]

The presence of Cu in 7xxx Al alloy has an intense effect on SCC behavior. Cu-rich grain boundary precipitates will cause lower electrochemical activity and lowers the hydrogen generation rates. Also, the dissolution of Cu both in matrix and  $\eta$  phase makes them noble where hydrogen generation accompanies the electrochemical dissolution at active sites in 7xxx alloys, resulting in an improvement of SCC resistance [30]. The GBP Cu content has effects on crack over-potential for H production and H trapping in the GB region. More Cu in the GBP (arising from optimized  $S$ -phase dissolution) raises the bulk alloy potential and makes the kinetics of hydrogen evolution more sluggish. It is also reported that increasing the Cu content of 7xxx alloys from 0.01% to 2.0% (mass fraction) declines the crack propagation speed progressively and the reduction reaches two orders of magnitude as a result of the change in the electrochemical activity of the  $\eta$  precipitates as a function of Cu content in alloys. The effects of Cu:Mg ratio on microstructure and properties of AA7085 alloys was studied by WU et al [31]. They observed that better recrystallization inhibition and corrosion resistance can be achieved when Cu:Mg ratio is 1.6. When Cu:Mg ratio is 0.67, the alloy reveals better mechanical properties, and the tensile strength and yield strength of AA7085 alloys are 586 and 550 MPa, respectively. Moreover,

both the mechanical properties and corrosion resistance of the alloy are reduced when Cu:Mg ratio is equal to 1.0.

Stress corrosion cracking (SCC) of two lower copper Al-Zn-Mg-Cu alloys, AA7079 and AA7022 (0.6%–0.9%Cu), and a higher copper AA7075 (1.5% Cu) alloy was investigated by KNIGHT et al [32]. In aqueous chloride, copper content of grain boundary precipitates is believed to be controlling, whereas in moist air, it appears that the hydrogen diffusivity could be evident from the rate of crack growth between crack arrest markings. In moist air, the rate of hydrogen entry may control crack growth rates [32].

It is reported that chromium and copper additions to the base alloy slow down the rate of pre-exposure embrittlement. Chromium slows down the transportation of hydrogen ions at the grain boundaries, hence increases the SCC resistance when alloys are pre-exposed to hydrogen containing corrosive environments. Alloying with chromium also reported that it forms much finer grains resulting larger grain boundary area which may reduce rate of hydrogen embrittlement [33].

The addition of the Sc in 7xxx alloy has beneficial effect on the strength and SCC behavior which is reported by CHEN et al [34]. It was observed that Sc in combination with Zr enhances the recrystallization inhibition effect significantly. It was also observed that the addition of Sc enhances the SCC resistance of Al-Mg alloys and Al-Zn-Mg-Cu alloy. According to Ref. [35], electrical conductivity factor was used as an index for evaluating corrosion resistance, that is, higher electrical conductivity means that the material has superior SCC resistance. LIU et al [36] stated that rare earth metals such as Er added to Al-Zn-Mg-Cu alloy and followed by heat treatment will enhance ductility, strength and conductivity, thereby increasing SCC resistance of the alloy [36]. The additions of Sc and Zr to Al-Zn-Mg-Cu alloy can improve the corrosion resistance observably due to the inhibition of recrystallization behavior. It was observed that the discontinuity of precipitates distribution along the grain boundary was enhanced by the introduction of Sc and Zr. Aged at 120 °C for 36 h, the Al-Zn-Mg alloy microalloyed with 0.25% Sc and 0.10% Zr exhibits high mechanical properties and admirable corrosion resistance [37].

Furthermore, addition of elements like Yb, Cr and Zr to Al-Zn-Mg-Cu alloy can highly improve the resistance to recrystallization and stabilize the deformation recovery microstructure by developing of low angle sub-grain. Addition of these elements also helps the growth of discontinuously distributed  $\eta$  phase particles at the grain boundaries of the unrecrystallized grains which have ability to enhance the resistance to

stress corrosion cracking, ductility, fracture and toughness and strength [34]. The combined additions of Zr, Er and Cr to Al–Zn–Mg–Cu alloy led to the formation of coherent Zn, Mg, Cu, Cr containing  $\text{Al}_3(\text{Zr,Er})$ . The secondary precipitates remarkably inhibited the recrystallization of Al matrix, and numerous fine subgrain boundaries were retained. Compared to the partial recrystallized Al–Zn–Mg–Cu–Zr alloy, the unrecrystallized Al–Zn–Mg–Cu–Zr–Er–Cr alloy exhibited higher resistance to intergranular corrosion and stress corrosion with the improved mechanical properties and fracture toughness [38].

Iron and silicon are reported to be the main impurities in commercial grade aluminium alloys [39,40]. The solubilities of iron and silicon are high in molten aluminum, but are low in solid aluminium [40]. Therefore, most of iron and silicon will precipitate out during solidification and form large second phase particles. The iron-rich particles, such as  $\text{Al}_3\text{Fe}$  and  $\text{Al}_7\text{Cu}_2\text{Fe}$ , usually act as cathodes on the surface of the alloy, promoting electrochemical attack. MURRAY et al [41] reported that the presence of Cu ions in the solution would cause metallic copper to plate onto the iron-rich particles. If the matrix adjacent to the iron-rich particles contains copper, aluminium will be dissolved and the copper will remain inside pits and plate onto iron-rich particles, which makes the particles more cathodic with respect to aluminium [41].

Evolution of microstructure and stress corrosion cracking (SCC) susceptibility of 7050 aluminum alloy with 0.094% Si, 0.134% Si and 0.261% Si (mass fraction) in T7651 condition have been investigated by HUAN et al [42]. The results show that the area fraction of  $\text{Mg}_2\text{Si}$  increases from 0.16% to 1.48% and the size becomes coarser, while the area fraction of the other coarse phases including  $\text{Al}_2\text{CuMg}$ ,  $\text{Mg}(\text{Al,Cu,Zn})_2$  and  $\text{Al}_7\text{Cu}_2\text{Fe}$  decreases from 2.42% to 0.78% with Si content increasing from 0.094% to 0.261%. The tensile strength and elongation of 7050-T7651 alloys is decreased with the increase of Si content by slow strain rate test (SSRT) in ambient air. However, electrical conductivity is improved and SCC susceptibility is reduced with the increase of Si content by SSRT in corrosion environment with 3.5% NaCl solution.

It can be concluded that Mg has adverse effect on the SCC initiation and its presence enables two mechanisms to activate SCC failures that provide an active path for diffusion of hydrogen ion into the grain boundaries and lead to intergranular cracking and it increases the anodic dissolution rate. To deactivate or to retard both the mechanism, it is reported that alloying with copper which dissolves in the matrix and enters the  $\eta$  phase along the grain boundaries, making both nobler. As a result, the mixed potential at the crack tip shifts to a

nobler value and hence SCC resistance is increased by reducing anodic dissolution rate and by reducing hydrogen diffusion rate. Similar observations are made with the addition of chromium.

## 2.2 Effect of microstructure and heat treatments on SCC behavior

The microstructural analysis of the alloy is the well evaluated parameter used to find the microstructural resistance to SCC without disturbing the high-performance mechanical properties of the material [43].

In 7xxx series aluminum alloy, highest strength attained in peak age heat treated conditions at T6 temper. High strength and mechanical properties in this temper condition are attributed to the presence of fine dispersed precipitates in the grains which obstruct the dislocation movement thereby enhancing the properties. The general precipitation formation sequence of 7xxx series alloys is solid solution  $\rightarrow$  GP zone  $\rightarrow \eta'$  metastable (semi coherent)  $\rightarrow \eta$  stable (pseudo coherent).

In peak aged condition, the main precipitates formed to be  $\eta'$  ( $\text{MgZn}_2$ ) or  $\text{Mg}(\text{ZnCuAl})_2$  which appears as distinct platelets particles that are semi coherent with the matrix. During aging, generally two aging peaks will be observed for the Al–Zn–Mg [44]. First aging peak is associated with coherent high density GP zones in the matrix. These GP zones are weak and soft and the strength of the first peak stage significant depends on density of the GP zones. Further increase in strength is attributed to the increase in surface energy when a dislocation bisects the GP zone. On further aging, the strength decreases due to dissolution of GP zones. The second peak is associated with semi coherent  $\eta'$  phase. In this stage, the dislocations only can bypass the  $\eta'$  phase (Orowan mechanism) [45]. According to the Orowan mechanism, the volume fraction of the  $\eta'$  precipitates and its interspacing will determine its peak value of the second peak. For instance, larger volume fraction of the precipitates and smaller interspacing will result in higher strengths. For 7xxx-T6 peak aged condition, the  $\eta'$  phase is the main precipitate and for the over-aged temper (T7x), the  $\eta$  phase is the main precipitate.

It was reported that the three regions in the microstructure play a critical role in SCC to occur, those three regions are 1) precipitates in the interior of the grain boundary, 2) the equilibrium precipitate lying along the grain boundary and 3) precipitate free zone (PFZ). The precipitates mentioned above are formed with proper heat treatment processes such as underaging, overaging, peakaging. and with proper assistances of quenching techniques and or formed with proper thermo-mechanical treatments. Aluminum alloys consist of large number of alloying elements which are differing in electrochemical potentials among themselves and also



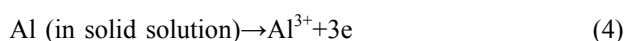
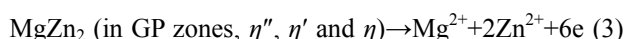
differ from the matrix. High strength Al alloys [46] contain two types of constituent particles which are contributed to high strength and SCC behavior. Those are 1) particles such as Al, Mg and Zn which are anodic with respect to the matrix and readily suspend, 2) particles behave as cathodic with respect to the matrix and tend to promote corrosion or disintegration of the adjoining matrix such as Fe, Cu and Mn. The presence of these two distinct categorized constituent particles tends to arise galvanic effect which results in development of corrosion pits at these particle interfaces. Once corrosion pits are formed, they act as sites for stress concentration, leading to stress corrosion cracking failure.

As 7xxx series aluminum alloys are extensively utilized in aerospace, structural components and in unique navy application, are subjected to aggressive environmental and stressed conditions where they encounter salt water spray and or salt fog environments. As in case of peak-aged condition, it has been observed that fine  $\eta'$  precipitates are dispersed inside the grains as well as at continually dispersed along the grain boundary. The grain boundary precipitates are identified as the equilibrium  $\eta$  ( $\text{MgZn}_2$ ) phase [47]. Due to the formation of different precipitates in and around the grain boundary, the potential difference between the matrix and grain boundaries raises. This continuous precipitate at the grain boundaries acts as anodic tunnels of intergranular corrosion and enhance the SCC rate of the alloy by accelerating the hydrogen transportation which further embrittles the grain boundaries [30]. In 7xxx Al series, the SCC mechanism involves repeated sequences of 1) generation of hydrogen at crack tips; 2) diffusion of hydrogen ahead of crack tips; 3) “brittle” fractures when a critical hydrogen concentration is reached over a critical distance.

A clear explanation of the correlating corrosion mechanisms to the microstructure was given by LIN et al [21], they have stated that the  $\text{MgZn}_2$  phase behaves as the anode and the oxide or the solid solution acts as the cathode.  $\text{MgZn}_2$  precipitates having the following factors such as coherency, nativity (matrix or grain boundary) and size will determine the electrochemical corrosion behavior of the alloy, thus have severe effect on the corrosion potentials. In the salt solution, Zn and Mg associate to the elements which are more electrochemical active than aluminum. In solid solution containing Zn and Mg, the corrosion potential of aluminum shifts towards the active direction. Further, Zn and Mg diffuse from the matrix to grain boundaries, resulting in diminishing the concentration levels of  $\text{MgZn}_2$  in the solid solution. Depletion of Mg and Zn in the matrixes results in a noble shift in the corrosion potential. The higher extent in precipitation of  $\text{MgZn}_2$ , the more the shift of corrosion potential to noble

direction.

The dissolution behavior of a specimen also influences the variation of corrosion potentials. The consumption by dissolution out of the active compound (such as  $\eta$  precipitates) in the specimen results in a shift of the corrosion potential to noble direction. Besides the dissolution of  $\eta$  precipitates from grain boundaries, coherent precipitates  $\eta''$ , semi-coherent precipitates  $\eta'$  and Al in the matrixes are dissolved into the solution with a simultaneously cathodic reaction. The anodic dissolution reactions are



And the simultaneously cathodic reaction is



The grouping of the cations (such as  $\text{Mg}^{2+}$ ,  $\text{Zn}^{2+}$  and  $\text{Al}^{3+}$ ) dissolved close to anodes leads to combination with the hydroxide in the vicinity of cathodes to form precipitation as their solubility product over the  $K_{\text{sp}}$  (equilibrium solubility product). Once the corrosion product produced on the specimen surface, it may prevail over dissolution behavior to dominate the corrosion and SCC phenomena.

There are two methods to improve the SCC resistance. The first method is to disintegrate the continuity of the GBPs and the second method is to decrease the potential difference between matrix and grain boundary. The extensive study of ARDO and TOWNSEND [48] stated that the dispersion or the arrangement of the matrix precipitate, size and type are very important in ascertaining the SCC behavior and also reported that the susceptibility changes with variation in the dislocation–matrix precipitate interactions and the width of the PFZ, which is immaterial in the SCC susceptible, the changes in grain boundary precipitates could have a perceptible effect on the SCC. Many researches attempted to change the in-grain and grain boundary precipitates by employing various thermal treatments. PUIGGALI et al [49] in their research observed that prolonging aging of French alloy 7010 increases the SCC resistance. This behavior is due to the alternating distribution and volume fraction of  $\text{MgZn}$ , also they stated that extended aging has clear influences on the growth and stability of the passive layer which has a tremendous effect on the inclination to pitting and intergranular corrosion and crack initiation, hence it can be concluded that microstructural features affecting the SCC resistance are the grain boundary precipitates (GBP). The other method for improving the SCC resistance is by increasing both the size and the inter-particle distance of the GBP [21]. SUN et al [50] correlated between grain boundary precipitates (GBPs)

area fraction and stress corrosion cracking (SCC) susceptibility for an Al–Zn–Mg alloy. They observed that the SCC susceptibility of the Al–Zn–Mg alloy first decreases and then increases with the increase of GBPs area fraction. And, SCC susceptibility of the Al–Zn–Mg alloy is dominated by hydrogen induced cracking when GBPs area fraction is relatively low and is dominated by anodic dissolution when GBPs area fraction is relatively high.

It is well known that precipitate free zones (PFZ) form during aging of high strength Al alloys. Various factors such as aging temperature, grain boundary mis-orientations and quenching rate from solution treatment have an influence on the PFZ width. Although there exists a significant microstructural difference between the PFZ and the adjacent matrix, it was reported that the width of PFZ ternary Al–Zn–Mg alloys has no influence on the SCC behaviour in aqueous sodium chloride solution [43]. However, the relative strengths of the PFZ and grain interior determine the extent of strain localization at grain boundaries and affect the fracture toughness [51].

Many investigations have correlated the size and/or composition of precipitate free zones (PFZ) and/or solute depleted zones (SDZ) adjacent to the grain boundaries to SCC performance [52,53]. The explanations provided for the influences of PFZ's and SDZ's contradict one another. Most of these studies indicate that the importance of the PFZ or SDZ is electrochemical. However, THOMAS and NUTTING [54] observed that intercrystalline mechanical fractures of Al–Zn–Mg–(Cu) alloys in peak-aged condition were associated with preferential slip in the PFZ. They hypothesized that the stress concentration effects at the grain boundaries combined with the “soft” PFZ may allow dislocation movement to take place in the PFZ at stresses well below the macroscopic yield stress. MCEVILY et al [52] also observed that the softness of the PFZ enhances localized plasticity at the grain boundary. Other studies indicate that they see no correlation between PFZ composition or width and SCC resistance [55]. The inconsistency of correlation between PFZ's and/or SDZ's and SCC resistance implies that while a PFZ may be a contributing factor in some instances, they may not be an essential microstructural feature in the EIC mechanism.

TSAI and CHUANG [56] studied the effect of grain size on the SCC behaviour of 7475 Al alloy. They observed that the refinement of grain attributed to attaining high homogeneous slip mode and has resulted in smaller sized grain boundary precipitates (GBPs), which have greatly influenced the SCC resistance. It was also reported that the high homogeneous slip mode is advantageous for enhancing the SCC resistance. However, if the size of GBPs was smaller than the

critical precipitate size for nucleating hydrogen bubbles, there is no beneficial effect due to either grain refinement or more homogeneous slip mode. The orientation of the grain also has influences on the SCC behaviour of high strength Al alloys. Intergranular SCC failures are very common in high strength Al alloys containing pancake shape grains, typically occurring in rolled plates and extrusions (Fig. 9). The failures occur predominantly when the applied stresses are in the short-transverse direction. However, when the applied stresses are in the longitudinal or long-transverse directions, the intergranular crack path is not easy, hence leading to a high resistance to SCC. Although transgranular cracking can occur when there is no easy intergranular pathway, it is not that widely reported.

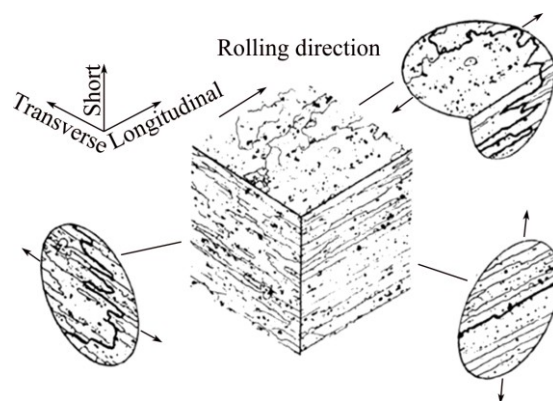


**Fig. 9** Effect of grain structure on intergranular crack for sample stressed in different orientations [5]

As stated earlier, peak aged condition (T6) of 7xxx alloy attains high strength and high mechanical properties due to precipitate hardening and has low response to SCC. Apart from peak aging, another aging treatment known as overaging (T7x) has significant response to SCC resistance when compared to T6 condition. In comparison with T6 condition, T7x temper condition is followed by loss in strength by 10% to 15% and reported lower hardness values due to coarsening of precipitates as it is exposed to prolonged heating. In this over aged state, the precipitates tend to coarsen and accumulate along the grain boundaries, which is potential to decrease the scattering of electrons and attributing in enhancing the conductivity.

Also, these coarsened precipitates discourage the phenomenon of anodic tunnels of intergranular corrosion. The coarsened and discontinuous precipitates, arranged at the grain boundary with inter-particle spacing decrease the anodic dissolution speed and act as the entrapping regions for atomic hydrogen ions and produce molecular hydrogen bubbles to reduce the accumulation of the hydrogen ions at the grain boundaries [57]. Also, it is reported that SCC resistance is enhanced by means of

the more homogeneous slip mode and reduction of the slip planarity, due to increasing in size of matrix precipitate and the associated changes from GP zone to semi-coherent and in coherent precipitates. It has been reported that a single step aging to the T73 and T76 regarded as a best approach to increase the tensile strength and SCC resistance.

LIN et al [21] explained the SCC mechanisms with respective to the heat treatment. They have stated that SCC degradation of 7xxx aluminium alloy in saline environment is due to the three major mechanisms: 1) anodic dissolution (AD); 2) hydrogen-induced cracking (HIC), and 3) passive film rupture (PFR). The anodic AD dissolution commences immediately when the 7xxx Al alloy is immersed in the corrosive environment. Anodic dissolution takes place along the active  $\eta$  precipitates whereas HIC mechanism undergoes between space of  $\eta$  precipitates. Both the mechanisms of AD and HIC were reported to be severer in T6, as the rate of AD is much quick in attacking the continuously arranged fine precipitates and HIC is severer in regions that have close space precipitates. Apart from the T6 temper, overaging T7X and other novel heat treatments provide a slow rate of anodic attack due to space interruption between the large precipitates. The large precipitates facilitate entrapment of high accumulation of hydrogen and prevent their dispersion to cause SCC failure. Thus, the increasing of the size and spacing of the  $\eta$  particle decreases AD and HIC.

To overcome the problem observed in overaging, that is loss of tensile strength and decrease in hardness values as compared to T6 treatment, a novel heat treatment proposed by CINA [58] known as retrogression and reaging (RRA) was developed to enhance the SCC resistance of 7xxx alloys without considerable change in strength when compared to the T6 temper. The RRA treatment consists of annealing process of T6 sample at 180–240 °C for 5–2400 s called as retrogression, which was followed by re-aging implementing similar conditions as used for the original T6 aging. During retrogression, it was reported that the initial strength decreases due to reversion of GP zones and dissolution of small  $\eta'$  particles in the matrix, retrogression treatment and upon further aging result in an increase in strength of T6 treated sample [59].

VIANA et al [60] studied the microstructural characterization of 7075 Al in RRA temper and interpreted through calorimetric studies and stated that RRA provided large precipitations of the equilibrium  $\eta$  phase in the grains and in sub-grain boundaries, and continued to preserve distribution of fine  $\eta'$  precipitations within the grain. The grain boundary consists of coarser intermetallic particles place in irregular intervals and acts as hydrogen entrapping regions which locally decrease

the hydrogen concentration in the matrix around the grain boundary. In this treatment, the increase in strength is attributed to the increase in  $\eta'$  precipitates and its arrangement in the matrix which nucleate due to their reprecipitation. On the other hand,  $\eta$  precipitates at grain boundaries are large enough when compared to the retrogressed state. The TEM microstructures are shown in Fig. 10. The corrosion resistance and strength of RRA-treated samples are sensitive to the pre-ageing temperature and retrogression heating rate. With an intermediate pre-ageing temperature of 60 °C and a slow retrogression heating rate of 5 °C/min, RRA-treated samples can be tailored towards a good combination of both corrosion resistance and strength, owing to a smaller potential difference between grain-boundary precipitates and the matrix, and a larger volume fraction of strengthening precipitates in the matrix [61].

In a brief, RRA promotes coarse precipitation of the discontinuous equilibrium phase  $\eta(\text{MgZn}_2)$  at in the grains and subgrain boundaries which are incoherent with the matrix and result in a reduction of lattice distortion and an increment of the conductivity while maintaining a fine distribution of  $\eta'$  in the grain interiors. These coarse intermetallic particles then act as hydrogen trapping sites, locally reducing the hydrogen concentration in the matrix around the grain boundary [62].

The microstructure with high strength and resistance to SCC alloy consists of a large number of fine particles and the relative strength to SCC is determined by the amount of hydrogen trapping ability by numerous interphase boundaries. The microstructure changes while application of retrogression treatment has been extensively studied by XU et al [63]. They have elaborated the changes in the microstructure in three distinct regions as a function of retrogression time. Region I indicates short retrogression time, which results in dissolution of main constituents such as GP zones and small  $\eta'$  precipitates of microstructure present in T6 temper state. Region II shows the curve at longer retrogression time with matrix rich in Mg and Zn because the dissolution encourages the nucleation of new  $\eta'$  precipitates, while existing  $\eta'$  precipitates transform and grow to  $\eta$ . Furthermore,  $\eta$  precipitates that are majorly present at the grain boundary are coarsened and spaced with larger intervals. The main microstructural changes observed in Region II are indication of size and quantity of  $\eta$  and  $\eta'$  precipitates. Furthermore (Region III), increase in retrogression time results in overaging which has consequence in precipitates coarsening. The TEM images of the T6, RRA and T73 tempers are shown in Fig. 10. The arrangements of the precipitates at the grain boundary are described through these TEM images. In T6 condition, the precipitates disperse continuously

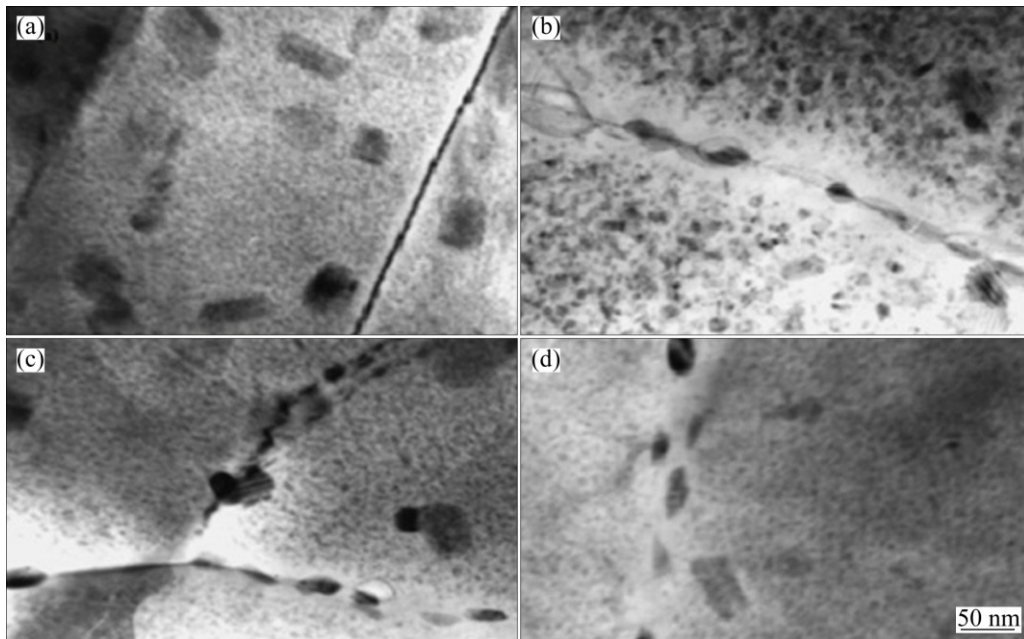


**Fig. 10** TEM images of 7075 alloy: (a) T6 temper; (b) Overaged T7 temper; (c) After retrogression; (d) After RRA [60]

alongside the grain boundary and finer precipitates are present inside the grains. In T73 condition, larger precipitates distribute discontinuously along the grain boundary while depleting distribution of the precipitates in the grain. Whereas in RRA-treated condition, the larger precipitates distribute along the grain boundary while maintaining the fine precipitates inside the grain which satisfy the both SSC and strength of the alloy.

LI et al [64] reported that RRA not only increases SCC resistance, but also increases the conductivity and in RRA treatment, with an increase in retrogression time and temperature, conductivity increases, while tensile properties decrease. Due to short period retrogression time, RRA treatment was only applicable for thin sections. Initially RRA was applicable for 1 to 6 mm thick components and the application of RRA to thicker components did not give good results. RAJAN et al [65] suggested that lower retrogression temperatures and longer retrogression time are achievable to apply RRA heat-treatment process to thicker components. And they also reported decreasing in hardness when retrogression is done for prolonged time due to excessive coarsening of the precipitates which is shown in Fig. 11. Hence, optimum retrogression temperature and time became challenging to fulfill both the strength and SCC in RRA treatment for thicker components.

FERRER et al [66] worked to determine the lower retrogression temperature used for RRA treatment to enhance the strength and SCC resistance and to extend the applicability of the low temperature retrogression to the thick section of 7075 Al alloy, aircraft components. They have concluded that lower retrogression

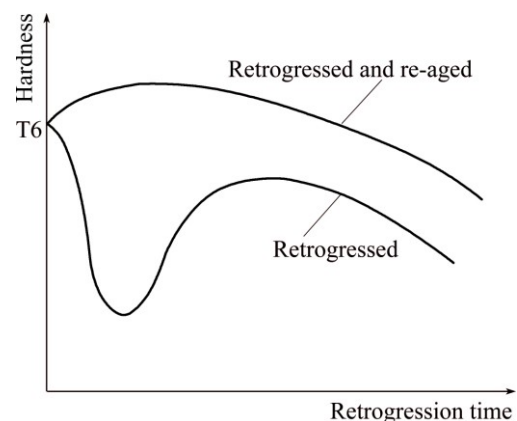


**Fig. 11** Schematic representation of change in hardness during retrogression and re-ageing [65]

temperature and longer duration can improve the SCC resistance of thicker sections by maintaining optimum strength. In this work, it was concluded that the RRA process with retrogression at 160 °C for 660 min resulted vast improvement in SCC resistance, with only a 4% deduction in strength below T6 [66].

OLIVEIRA et al [67] studied the effect of RRA on the SCC resistance and strength of AA7050 alloy and AA7150 aluminium alloys and concluded that maximum hardness after re-aging was obtained in the samples retrogressed for 20 and 40 min. After RRA process, 30% improvement in the yield strength was observed in the AA7050 alloy, while for AA7150 alloy, the mechanical properties were similar to those under the original condition and SCC for both alloys after RRA for 40 min showed the same pattern as of original condition.

Many researchers worked to improve the SCC

resistance by implementing various thermal treatments on the 7xxx alloys, some of the novel thermal treatments are reported below. Apart from aging treatments on the effect of microstructure behavior on SCC, solution treatment also has an impending effect on the microstructural evolution and the SCC behavior. SONG and CHEN [45] reported that in the Al–Zn–Mg alloy, enhancement in SCC resistance can be achieved through improved solution heat treatment and high temperature pre-precipitation process. In this combined process, high Cu concentrations and low Mg can be attained with arrangement of discontinuous distribution of GBPs. It was confirmed that altering the solution treatment temperature has influence on the stress corrosion susceptibility by changing the metallurgical microstructure and the grain boundary composition [68]. The GBPs concentrations of Cu, Mg and Zn depend on the solution heat treatment temperature. As the solution heat treatment temperature decreases, the mentioned concentration also decreases. It was also reported that solution treatment temperature also has influence on the stress corrosion plateau crack velocity.

JOSHI et al [69] have determined that the amount of constituent particles such as Mg, Zn, Cu, Fe and Si at the grain boundary depends on the solution heat treatment and successive annealing treatment. They also reported that if identical solution heat treatments are involved, the final aging treatment influences the grain boundary solute distribution. They have observed that at 438 °C, the solute concentration was minimum at solution heat treatment done in the range of 399 to 527 °C [69].

Stepped solution treatment also has a remarkable influence on the SCC behavior and strength of the alloy. The multi stepped solution treatment, prior to RRA treatment increases the dissolution of *S*-phase (Al<sub>2</sub>CuMg) which increases the copper content at the grain boundary and increases the SCC resistance by retarding the anodic reaction kinetics.

XU et al [30] studied the effect of *S*-phase dissolution on the corrosion and stress corrosion cracking of an as-rolled Al–Zn–Mg–Cu (AA7150) alloy and concluded that high temperature stepped solution treatment can effectively release Cu into the matrix which increased the Cu content at the grain boundaries after RRA treatment [30]. Another novel heat treatment well-known as multi step aging combined with controlled heating rate to attain the final over-aging temperature. This novel heat treatment resulted in better combination of improved strength and fracture toughness. As the RRA treatment was restricted only to the thinner sections whereas this novel multi-step aging is more advantageous and can be applicable to thicker sections. BOBBY-KANNAN et al [11] reported that with this novel treatment, sample can attain superior SCC

resistance with higher ductility in Al–Zn–Mg–Cu–Zr alloy.

Interrupting aging T6I6 (130 °C, 80 min + 65 °C, 240 h + 130 °C, 18 h) was studied by LI et al [70] compared with the precipitate densities formed conventional aging treatment such as T6, T7X, RRA and stated that T6I6A possesses high density of  $\eta'$  precipitates than the T6 and other aging processes and that RRA and T6I6 maintain the strength as that of T6 state and with increase in SCC resistance as compared with T73 and HTPP treatments [70].

REDA et al [23] and BAYDOGAN et al [63] worked to increase the strength, hardness and resistance to SCC of 7075 Al alloy by considering different combinations of pre-aging and retrogression temperature for different durations of time. They have concluded that the optimum condition was preaging at 120 °C and retrogressing at 200 °C, which gave the highest hardness and tensile properties. Preaging at 100 °C and retrogression at 160 °C for 250 min resulted in high resistance to SCC and the sample retrogressed at 200 °C for 8 min resulted in low stress corrosion cracking resistance. They have also reported that the sample retrogressed between 170 °C and 240 °C for short span of time resulted in superior combination of hardness and SCC resistance than the T6-temper state. Further, high retrogression temperature of 380 °C resulted in reduction in SCC and mechanical properties. They concluded that sample retrogressed at 170 °C resulted in excellent combination of SCC and with 20% enhancement in hardness and 85% improvement in resistance to corrosion.

SILVA et al [71] studied the effect of heat treatment parameters on improving the tensile strength and SCC resistance of 7075 Al alloy. They conducted the test on variously aged sample such as T6, T73, T76 and aged at 163 °C for different durations of time (3, 5, 8, 16 and 24 h). Their main aim was to study the tensile properties and the SCC behavior of 7075 thick plates when submitted to a single step aging by varying the ageing times and to decrease the production cost to produce an aircraft material. They concluded that T76 treatment can be replaced by aging at 163 °C for 8 h for larger plates. T6 plates aged at 163 °C for 3 and 5 h showed failures to SCC. While T76, T73 and plates aged at 163 °C for 8, 16, 24 h showed no failure to SCC which can be interpreted in Fig. 12 [71].

Aside from heat treatment, quenching rates also play an important role in an organization the constituent particles in high strength Al alloys. It has been stated that high strength 7xxx alloys are quenching sensitive and many authors studied the effect of quenching rates on the mechanical properties and SCC behavior. It has been



reported that decreasing the quenching rate will increase the size and inter particle distance of the GBP along with increase of width of PFZ. Unfortunately, the copper percentage in grain boundary precipitates will decline with decrease in quenching rates. The resistance to SCC of the material first increases and then decreases, attributing to the distribution and size of GBP and copper content at GBP.

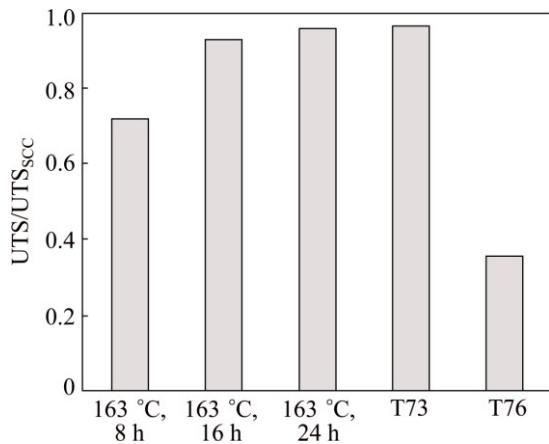


**Fig. 12** Ratio between ultimate tensile stresses obtained from tensile tests and ones obtained by tensile loading of corroded specimens [71]

Recently, OU et al [72] and LIN et al [21] have developed new heat treatment known as step-quenching aging (SQA) and stated that this method has ability to enhance the SCC resistance without losing its strength. OU et al [72] also studied effect of step homogenization on the mechanical and SCC behavior of 7050 Al alloy shown in Fig. 13. They have concluded that the densest and finest distribution of dispersoid, produced through step homogenization (Step-H) treatment, can efficiently inhibit recrystallization to attain the structure which contains smallest fraction of recrystallization. And step quenching and aging develop

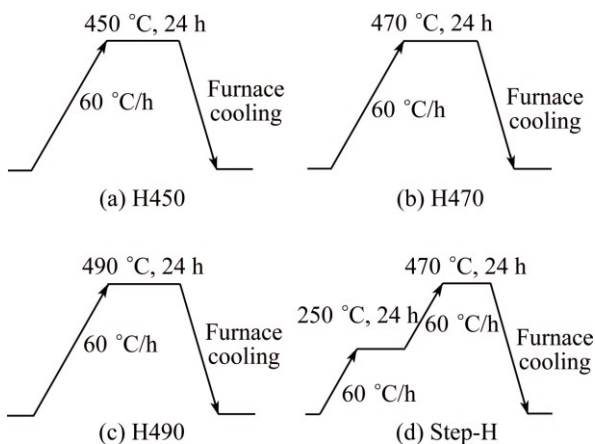


**Fig. 13** Schematic representation of different homogenization (H) treatments [72]

broad spaced GBPs which increase SCC resistance [21,72].

Many authors studied the effect of heat treatment and arrangement of the microstructural constituents of the alloy on the SCC behavior and concluded that overage, RRA and novel treatments such as multi-stepped aging and solutionizing treatments are beneficial to improving the SCC without loss of mechanical properties. As these treatments provide efficient arrangement of microstructural constituents which will retard the mechanisms of hydrogen induced cracking and anodic dissolution which are the most widespread in 7xxx series alloys.

### 2.3 Effect of stress on SCC behavior

Stress raisers of flaws (such as bolt holes, fatigue cracks, notches etc.) are often required to imitate SCC failure. The magnitude of the stress field surrounding a stress raiser, the stress intensity factor ( $K$ ), is a function of the flaw size ( $a$ ), applied stress ( $\sigma$ ) and other geometric considerations that depend on the configuration and the manner the stress is applied. Generally, double cantilever beam (DCB) specimens which resemble as fatigue pre-cracked specimens used to measure stress corrosion crack propagation rates, are designed to maintain plane strain loading conditions.

MAGNIN [73] made some interesting observations comparing stress corrosion cracking (SCC), which occurs under sustained tensile loads and/or at slow strain rates and corrosion fatigue (CF) which occurs under cyclic or dynamic loading conditions. At the free corrosion potential, corrosion fatigue occurs at all strain rates from  $1 \times 10^{-8}$  to  $1 \times 10^{-2} \text{ s}^{-1}$  unlike SCC, which only occurs at strain rate  $< 2 \times 10^{-5} \text{ s}^{-1}$  for 7020-T4 UA and  $8 \times 10^{-7} \text{ s}^{-1}$  for 7020 OA (T6DR). At strain rates  $> \epsilon$  (SCC), transgranular corrosion fatigue microcracks are formed by a combined effect of breakdown of the passive film and due to plastic strain localization fatigue. At strain rates  $< \epsilon$  (SCC), intergranular microcracks can be formed by SCC, and CF is enhanced by SCC. However, if a cathodic potential ( $-1100 \text{ mV vs SCE}$ ) is immediately imposed upon exposure to the electrolyte, SCC does not occur because micro-crack formation requires anodic dissolution. Corrosion fatigue occurs by H entry and embrittlement at mechanically formed micro-cracks. These observations support the necessity of a surface defect for hydrogen entry. For SCC, the surface defect is created by anodic dissolution while in CF the surface defect is created by mechanical means. It was therefore proposed by MAGNIN [73] that anodic dissolution contributes mainly to initiation phase and hydrogen to the propagation phase.

TIEN et al [74] proposed dislocation sweep model which predicts a critical strain rate proportional to the

critical velocity at which the dislocation line would be expected to break away from its hydrogen cloud so that dislocation sweeping is no longer effective. In this model, the embrittlement would be proportional to the strain rate at strain rates below the critical strain rate. The data are consistent with the TAHERI et al [75] evaluated strain rate dependence of hydrogen embrittlement for three conditions (under aged temper = UT, T6 and T73) after cathodically pre-charging in HCl solution (pH=1). Strain rates ranging over 4 orders of magnitude reported that all three tempers exhibited a maximum in embrittlement (based on reduction in area, RA) at intermediate strain rates. The strain rate of maximum brittleness increased with degree of aging as illustrated in Fig. 14. The explanation provided was that at low strain rates the accumulation of hydrogen atoms at trap sites is reduced by diffusional escape and at high strain rates the hydrogen atoms can neither diffuse nor be carried by dislocations [75].

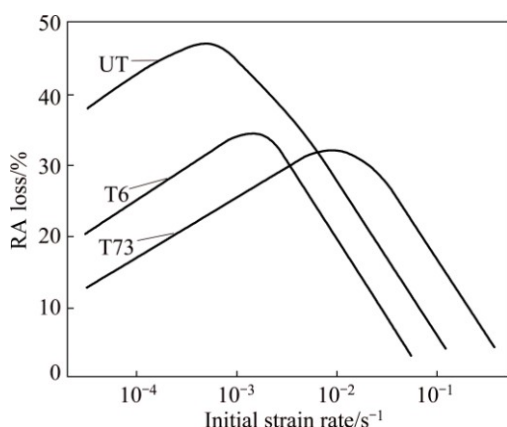


**Fig. 14** Loss of reduction in area (RA) in hydrogen charged specimens as function of strain rate [75]

## 2.4 Effect of environment on SCC behavior

As stated earlier, composition, heat treatment and microstructure of the material play a major role in SCC susceptibility, but little change in the composition of major alloying elements such as Mg and Zn or ratios of them can drastically alter the SCC behavior. Aluminum alloys are prone to corrosion in  $\text{Cl}^-$ ,  $\text{Br}^-$  and  $\text{I}^-$  aqueous solutions and also in moist air and in distilled water. In generally, 3.5% NaCl solution is taken as corrosive environments for aluminum alloys as it is believed to result in severe general corrosion rates and it represents roughly the salinity of sea water. As aircrafts are exposed to several complex chemical environments both inside and outside, no single environment could simulate the actual condition for this reason, 3.5% NaCl solution is taken as a corrosive environment as it assumed as “realistic chemical corrosive environment” [76]. It is also stated that high strength aluminum alloy containing copper in 3.5% NaCl aqueous solution develops severe

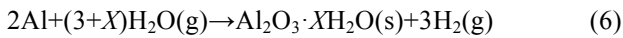
pitting and finally leads to mechanical failures. Apart from 3.5% NaCl aqueous solution, many synthetic environments such as simulated sea water were used to study SCC behavior. BRAUN [77] studied the effect of various synthetic environments on the SCC behavior of 7050 Al alloy by using SSRT technique and concluded that 7050-T7351 alloy shows high resistance to SCC, T6 condition shows a less resistance and when tested with an aqueous solution of 0.5 mol/L  $\text{NaClO}_4$  on a smooth specimen, no SCC was observed. Al 7050-T651 alloy was found to be sensitive to environmental assisted cracking when performing SSRT in an aqueous solution of 0.1 mol/L NaCl + 0.05 mol/L  $\text{Na}_2\text{SO}_4$  + 0.05 mol/L  $\text{NaNO}_3$  + 0.01 mol/L  $\text{NaHCO}_3$  at pH 3.5. This synthetic environment did not promote IGSCC when the alloy was aged to the tempers T7651 and T7351.

In high strength aluminum alloys, crack velocity of the alloy may increase over nine orders of magnitude depending on the environment. The environment has a vital effect on the initiation and propagation of subcritical stress corrosion cracking. A severe SCC failure takes place in cyclic wet/dry exposure to corrosive environment as compared to constant immersion conditions where other forms of corrosion such as pitting dominate.

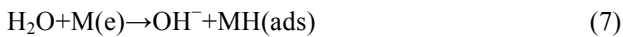
The importance of the wet dry cycles for SCC has generally been attributed to the concentrating of aggressive ions such as chloride ions. This transition from SCC susceptibility under intermittent exposure conditions to pitting in constant immersion exposures implies that a particular balance between anodic dissolution and passivity may be important to the SCC mechanism.

SCC susceptibility was only observed in humid and moist environments and it was absent in the dry air conditions such as in argon and in nitrogen. The plateau or Stage II crack growth rate (stress-independent crack growth rate) is  $\sim 2.5 \times 10^{-3}$  cm/h in the moist gases at 100% relative humidity. The analogous crack growth behavior in various gaseous environments indicates that the water vapor causes SCC of high strength aluminum alloys. Tests on 7075-T651 alloy at varying levels of RH in air have shown a linear dependence of crack growth rate on the log (RH) as illustrated in Fig. 6. In Stage I, the crack growth rate increases with increase in the applied stress intensity until the crack growth reaches a rate that is reaction limited and crack growth rate remains relatively constant with further increase in stress intensity. The dependence of the plateau crack growth rate on water vapor content implies that the transition from Stage I (stress-dependent) to Stage II (stress independent) crack growth is due to a reaction or process kinetic limitation related to the available water vapor [26].

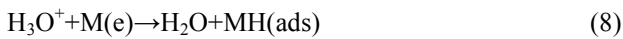
SCC failure reported in high humidity environments is apparently due to the reaction between the aluminum and water molecule to form high fugacity hydrogen gas through the overall reaction:



In this reaction hydrogen gas evolved, the reaction actually occurs in multiple steps [78]. The first step is generally an electronation reaction. The reduction of water at the oxide metal interface produces atomic hydrogen, which can either be absorbed into the metal or recombine to form  $\text{H}_2$  gas.



In neutral to acidic aqueous solutions, the electronation reaction can occur by proton discharge, i.e., reduction of hydrated protons:

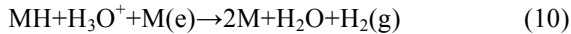


The recombination of adsorbed hydrogen can occur by two possible types of paths. It can occur without charge transfer by chemical desorption or by means of an electrodic desorption step such as:

Chemical desorption:



Electodic desorption:



If the actual reaction path on a particular metal electrode involves a fast electronation reaction step followed by a slow (rate-determining) desorption step, adsorbed hydrogen atoms will accumulate on the metal surface and a high surface coverage of adsorbed hydrogen atoms will exist in steady state conditions. On the other hand, if proton discharge is slow, then the formation of adsorbed hydrogen is difficult and the hydrogen atoms that do arrive on the surface rapidly form hydrogen gas, so the surface coverage remains low.

The heat of absorption associated with the gas phase adsorption of atomic hydrogen is approximately equal to the strength of the metal-hydrogen bond [78]. For the transition metals, the bond strength is related to the d-band character of the metal. As the d-band character increases, the current density at cathodic overpotentials decreases, M—H bond strength increases, the hydrogen adsorption energy decreases, and coverage with hydrogen atoms increases. For metals with sp valence orbitals (no d electrons), the current density at cathodic overpotentials increases as M—H bond strength increases.

The exchange current density for the hydrogen-evolution reaction provides a relative measure of the reaction rate on a metal electrode [78]. Aluminum is a relatively poor catalyst for the hydrogen evolution

reaction with an exchange current density on the order of  $10^{-9}$  A/cm<sup>2</sup>. For 7xxx series alloys, the electronic nature of the various alloying elements in solid solution may significantly influence the exchange current density for the hydrogen evolution reaction. Zinc is a poorer catalyst than aluminum with an exchange current density on the order of  $10^{-10}$  A/cm<sup>2</sup>, which is consistent with the lack of unpaired d-band electrons in zinc. Copper on the other hand is a relatively good catalyst for the hydrogen evolution reaction with an exchange current density on the order of  $10^{-6}$  A/cm<sup>2</sup>. Therefore, zinc in solid solution could enhance the adsorption of hydrogen while copper in solid solution could significantly reduce the hydrogen absorption of the alloys. Accurate determination of the actual reaction path can generally be accomplished by a combination of the evaluation of the dependence of hydrogen coverage,  $\theta$ , on the electrochemical overpotential,  $\eta$ , and evaluations of the transfer coefficient (Tafel slope  $\alpha$ ), reaction order and reaction stoichiometry. Evaluation of these parameters on copper electrodes indicates a rate determining proton discharge mechanism with low coverage of the metal surface with hydrogen [79]. This reactivity of copper implies that one possible contribution of copper for SCC resistance of 7xxx alloys may be to reduce the adsorption of hydrogen, i.e., to catalyze recombination/hydrogen evolution.

Adsorbed hydrogen can either recombine to form hydrogen gas or diffuse into the metal. High surface coverage on metals for which the desorption step is slow favors hydrogen uptake in the metal because of the longer residence time. Numerous investigations have evaluated the diffusion of hydrogen in aluminum but with little agreement on the diffusivity and activation energy values.

Increases in temperature decrease the time to failure in SCC tests using smooth tensile bars. Quantitative measurements of crack growth rates in pre-cracked specimens as a function of stress intensity and temperature have shown that increasing the temperature generally increases the Stage II crack growth rate and sometimes shifts Stage I to lower stress intensities, i.e., decreases  $K_{\text{ISCC}}$  as illustrated for AA7079-T651 and AA7039-T651 in Fig. 15. In fact, if the logarithm of the crack growth rate ( $\lg(da/dt)$ ) is plotted versus reciprocal temperature, a linear relationship can be observed, indicating that SCC is a thermally activated process with characteristic Arrhenius behavior as illustrated in Fig. 16. Therefore, Stage II crack velocity is apparently related to temperature by the following general equation:

$$v_{\text{II}} = v_0 \exp[-Q/(RT)] \quad (11)$$

where  $v_{\text{II}}$  is the Stage II crack velocity ( $da/dt$ ),  $v_0$  is a pre-exponential experimental constant,  $R$  is the gas constant (8.314 J/(mol·K)),  $T$  is the temperature (K), and

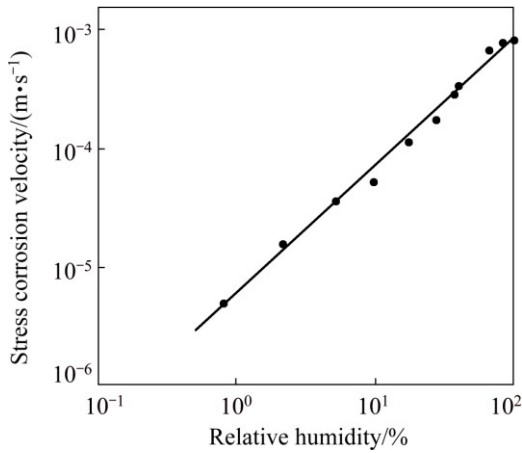


**Fig. 15** Illustration effect of humidity of air on stress independent crack velocity of high strength aluminum alloy [26]

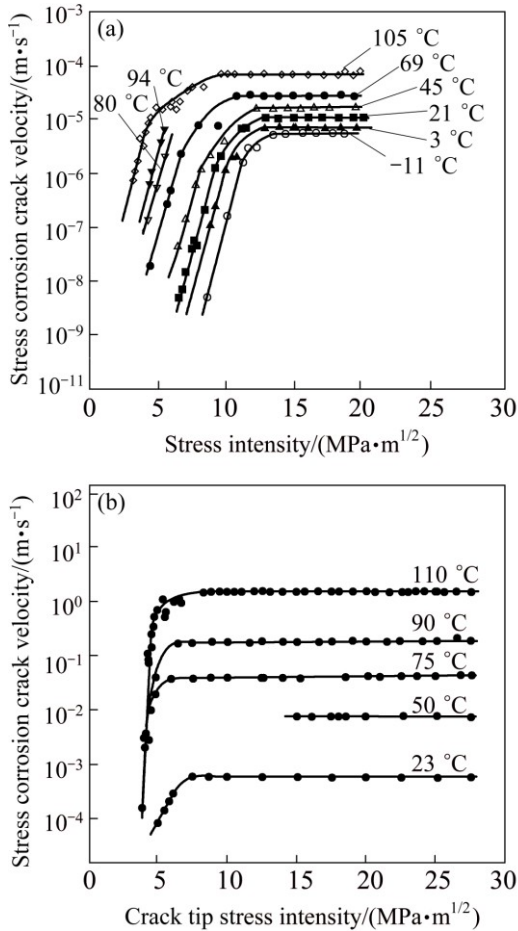


**Fig. 16** Effect of temperature and stress intensity on crack growth rates for 7079-T651 (a) and 7039-T651 (b) [26]

$Q$  is the apparent activation energy for crack growth. In Stage I, the crack velocity is dependent on both stress intensity and temperature as follows:

$$v_1 = v_0 \exp\left[\frac{-Q + bK}{RT}\right] \tag{12}$$

where  $v_1$  is the Stage I crack velocity ( $da/dt$ ),  $K$  is the

stress intensity, and  $b$  is an experimentally determined constant that is related to the crack tip geometry.

$$b = 2U/(\pi\rho)^{1/2} \tag{13}$$

where  $U$  is the activation volume and  $\rho$  is the radius of the crack tip curvature. These relationships imply that the stress dependence of the crack velocity should decrease as the radius of the crack tip curvature increases. Therefore, enhanced plastic relaxation of the crack tip should result in reduced stress dependence of crack velocity as yield strength decreases. For 7xxx alloys, this reduced stress dependence has been observed as a function of over aging time whereas decreases in yield strength corresponding with decreasing slopes in Stage I of the  $v$ - $K$  curve [26].

Stress corrosion behaviors in mode I (tension) and in mode III (torsion) of underaged, T6- and T73-treated 7075 Al in a corrosive medium of 1 mol/L  $AlCl_3$  were reported to be high resistance to SCC in T73 condition. MUELLER et al [80] reported that predominant mechanisms of SCC were hydrogen embrittlement in mode I and anodic dissolution in mode III. They also concluded that highly aggressive environment such as  $AlCl_3$  can add a strong non-SCC component to the cracking and therefore lead to possible misinterpretations of accelerated laboratory SCC tests conducted in this environment. A better suitable corrosive environment to conduct SCC test is an aqueous solution of 3.5% NaCl.

The effect of test environment temperature on SCC behavior was studied by ONORO and RANNINGER [81]. They stated that temperature of the environment is a basic parameter for the SCC process. And it has influence on the chemical reactions at the crack and also has influence on rate of diffusion of corrosion products from the corrosion environment to material. The SCC test was conducted in different test heated environments (20 and 80 °C) under different temper conditions and concluded that T6 condition has higher susceptibility to SCC than T73 and RAA.

Many authors have studied the effect of the moisture content on loss of ductility when SCC test was conducted in laboratory environment, and main emphasis was made on the presence of humidity and hydrogen presence in the laboratory environment and they have also studied the effect of relative humidity and found that the ductility ratio decreases with increase in relative humidity. SCC behavior of underaged 7010 Al was tested in glycerin and the results were compared with the results obtained from 3.5% NaCl solution and laboratory air [82]. It was concluded that laboratory atmosphere is not considered as inert atmosphere as the alloy undergoes SCC failure due to hydrogen embrittlement and due to relative high humidity of the test

environment. In contrast, they have concluded that glycerin can be taken as inert environment for conducting SCC.

TSAI et al [20] has studied the effect strain rate, solution pH and dissolved oxygen on SCC behavior of 7050–T7451 Al alloy in 3.5% NaCl solutions. They have concluded the following observations. At strain rate of  $8 \times 10^{-7} \text{ s}^{-1}$  in neutral 3.5% NaCl solution, the alloy was most susceptible to SCC in short transverse direction. Regardless the presence of dissolved oxygen at  $\text{pH} < 4$ , the alloy was more susceptible to intergranular stress corrosion cracking and at  $\text{pH} > 10$ , SCC was less convincing to failure as compared to acidic environments. But they observed that in the presence of oxygen in the pH range of 4 to 10, SCC is more profoundly affected. The alloy tested was susceptible to SCC in non-deaerated solution but showed immunity when oxygen was removed. The presence of oxygen would promote pitting corrosion and assisted the nucleation of stress corrosion cracks [20].

Effect of solution pH on electrochemical and stress corrosion cracking behavior of 7150 alloy was studied by ROUT et al [83]. Slow strain rate test (SSRT) results exhibited that highly over-aged temper has higher resistance to stress corrosion cracking (SCC) compared to that of underaged (T4) and peak aged (T6) tempers. Further, for all the alloy tempers, the SCC susceptibility was the most severe in solution pH 1, intermediate in solution pH 12 and the least in solution pH 7. And they concluded that local anodic dissolution (LAD) of grain boundary precipitates exacerbated by stress and accompanied by hydrogen induced cracking (HIC) are the probable mechanisms to induce SCC in the 7150 alloy in T4 and T6 tempers.

Extensive research has been done on the effect of the pre immersion on the stress cracking behavior of Al alloys, it has been stated that pre-exposing results in the diffusion of  $\text{H}^+$  ions through the grain boundaries which leads to decrease of the grain boundary cohesion in turn intergranular fracture due to hydrogen embrittlement. SCAMAN et al [33] observed same behavior of embrittlement of grain boundaries when working on the SCC behavior of pre-immersed 7075 Al alloys. The severity of hydrogen embrittlement depends on the factors such as pre-exposure time, temperature of the environment and relative humidity of the pre-exposure environment. They have also reported that the addition of copper up to 1.7% or chromium up to 0.14% suppresses the hydrogen embrittlement in high purity alloy and even more decreases in the 7075 Al alloy [33].

The surface of the sample becomes saturated with hydrogen when pre exposure with corrosion media and further upon application of stress causes this hydrogen to penetrate into the bulk of the specimen. The effect of

pre-exposure can be removed through repeating the complete heat treatment process as done to 7xxx Al, after exposed to the saline environment. Pre exposure of the corrosive media decreases the ductility of the commercial 7075 alloy due to pre-cathodic charging. As the pre-cathodic charging of this alloy exhibits all the aspects of typical strain aging hydrogen embrittlement. Similarly, TROMANS and PATHANIA [84] reported that the pre-cathodic charging also decreases the time to failure of stress corroded high purity 7xxx alloys in this aging attributing to the hydrogen embrittlement.

Pre immersion in 3.5% NaCl ( $\text{pH}=12$ ) about 240 h of various heat treated Al 7050 on the behavior on SCC was investigated by LIAO et al [22]. They observed that for a specific heat treatment, the pre-immersed sample shows high resistance to SCC than that of the sample without pre-immersion. In this research work, they have reported unpredicted result that peak aged condition shows high resistance to SCC and resistance decreases in overaged condition. In this work, they have observed that the passive  $\text{CuO}$  was observed when T6 sample was pre-exposed thus, attributing to high resistance to corrosion whereas a mixture of  $\text{CuO}$ ,  $\text{Cu}_2\text{O}$  and  $\text{CuCl}_2$  in aluminum hydroxide was observed for the RRA and step solutionizing treatments which results in degradation of the alloy. From the above perspective of the research work, it is concluded that the main mechanism behind SCC is attributed to hydrogen embrittlement. Much of the observation shows that similarities between pre exposure embrittlement and stress corrosion cracking (e.g., crack morphology, effect of solute additions such as copper and chromium and activation energy of the rate controlling process) strongly suggest that hydrogen embrittlement is the principal mechanism.

## 2.5 Effect of pre-strain on SCC

In order to relieve the quenching induced internal stresses, a pre-strain is generally applied to the as-quenched 7xxx series alloys. In the pre-strain process, the incubation of the dislocation network in the matrix takes place which provides efficient sites for heterogeneous direct nucleation of the  $\eta$  precipitates. They also provide fast diffusion paths for the precipitation elements in the further aging process and can significantly influence the sequence of precipitation which leads to strength to increase [85].

FOOLADFAR et al [86] has studied the novel treatment which included one shot-peening stage before or between the two stages of aging at  $120 \text{ }^\circ\text{C}$  for 24 h and at  $160 \text{ }^\circ\text{C}$  for 1 h, respectively and observed that the mechanical properties with this operation were similar to those of the T6 sample owing to the unaffected bulk microstructure over such a low over-aging period. This treated sample has higher SCC resistance than the T6



condition due to dislocations generated which change sequence of precipitate formation ( $GP \rightarrow \eta' \rightarrow \eta$ ). On further over aging, SCC resistance increased. They have reported that more depth of over-aging and the larger size and inter-particle space of the grain boundary precipitates increase SCC resistance of the shot-peened sample [86].

For the 7xxx alloys, the pre-strain usually resulted in the generation of the equilibrium phase  $\eta$ (MgZn<sub>2</sub>) on the dislocation network; therefore, it reduced the amount of the solutes for the formation of the main hardening phase  $\eta'$  in the T6 sample, leading to decrease in the mechanical strength of the alloys. The subsequent aging at above 160 °C makes the grain boundary precipitates enlarge and distribute discontinuously. Similar to the GBPs, the precipitates nucleate on the dislocations within the grains enlarged, causing the strength to diminish [9]. The dislocations generated during the pre-strain process are also of benefit to the solute element diffusion to the grain boundaries. The high density of dislocations is advantageous to the growth of the GBPs, and also decreases the width of the precipitate free zone (PFZ) via solute transfer from the grain interiors to the grain boundaries [87,88]. WANG et al [89] have studied the effect of severe cold rolling on the tensile properties and stress corrosion cracking of 7050 aluminum alloy and concluded that increase in cold reduction increases yield strength and UTS when compared to T6 condition. Furthermore, the enlargement in the size and particle interval of the grain boundary precipitates improved the stress corrosion crack (SCC) resistance of the cold rolled samples compared to that of the T6 sample [89].

NGUYEN et al [90] proposed that the increment of the precipitate size and the associated change from the GP zone to the semicoherent  $\eta'$  and incoherent  $\eta$  precipitates result in a more homogeneous slip mode and a reduction in slip planarity. That effectively decreases the mobile dislocation and, by a greater degree, brings down the hydrogen transported to the GB in the pre-strained samples.

## 2.6 Stress corrosion cracking of surface-treated 7xxx alloys

It has been reported that during the various heat treatments of the 7xxx aluminum alloys, several constituent phases are formed. The formation of these phases will vary in size and shapes. Generally, four types of coarser particles or phases are formed, i.e., AlSiZnCu, AlCuFeZn, AlZnCu, and AlCuZnTiSiCr, in 7xxx Al alloys. These coarser precipitates act as the pitting sites for corrosion and crack imitation.

Laser surface melting has been the subject of significant interest as a means of improving the corrosion

performance of aluminium and its alloys. Microstructural modification resulted from relatively rapid rates of cooling compared with conventional surface treatment techniques provides the basis for property enhancement.

YUE [91] studied the effect of excimer laser surface melting on SCC behavior. It was observed that in re-solidified laser-melted zone, the original grain boundaries were altered and the corrosion caused by coarse second-phase particles was eliminated. The new grain boundaries after re-solidification were free from precipitates which improve the SCC resistance. In addition to that, a layer of nanocrystalline structure of Al<sub>2</sub>O<sub>3</sub> had formed on the outer surface which retards the corrosion attack.

The pitting corrosion fatigue behavior of aluminium alloy 7075 after excimer laser surface melting was studied by CHAN et al [92]. LSM resulted in a reduction both in size and number of constituent particles and a alteration of the grain structure within the laser melted region resulted in improvement in corrosion. In dry fatigue condition, for LSM sample, the total fatigue life was lower than that of the untreated sample. Upon the shot peening of the LSM sample, the total fatigue life was enhanced. They also observed that the shot peened LSM sample tested in 3.5% NaCl solution with 48 h resulted in high total fatigue life than the untreated specimens with an increase of two orders of magnitude in fatigue life.

YUE et al [93] also studied the stress corrosion cracking (SCC) behavior in a 3.5% NaCl solution employing slow strain test on the 7075 aluminum alloy after excimer laser surface treatment. They have observed that the SCC initiation resistance of 7075 aluminum alloy was appreciably enhanced when tested in SSRT using 3.5% NaCl as corrosive environment. They also reported that for untreated specimen, brittle intergranular fracture was observed and transgranular fracture features were observed when both tested in anodic potential. They have also observed that laser treatment reduced the hydrogen evolution rate when tested under cathodic polarisation conditions.

Effect of Nd:YAG laser surface treatment of aluminum alloy 7075 was studied by YUE et al [94]. In this work, LSM was done under two distinct shrouding gas environments nitrogen and air. They observed that constituent coarse particles were eliminated and fine cellular/dendritic microstructures had formed and for the N<sub>2</sub>-treated specimen, an AlN phase observed to be present. They have concluded that the untreated sample resulted in intergranular crack. While laser treated sample lased without any shrouding gas resulted in long stress corrosion cracks along with small number of corrosion pits. These observations made when sample were immersed in corrosive medium for 30 d. While for

N<sub>2</sub> treated samples, few short stress corrosion cracks were observed attributing to enhancement in corrosion initiation resistance due to the presence of AlN phase which acts as insulator providing barrier for the corrosion attack.

Micro arc oxidation (MAO) treatment and plasma-electrolyte-oxidation (PEO) treatment improves the SCC resistance. Ceramic alumina coating by MAO and PEO method offers good barrier effect and improves elongation in chloride environments on meliorating the localized corrosion resistance of AA7075 aluminium alloy under long-term immersion conditions [95,96].

### 3 Stress corrosion cracking of weldments

Gas metal arc (GMA), plasma arc (PA) and gas tungsten arc (GTA) are widely used welding process to weld aluminium alloys. Fusion welding processes are used mostly for 5xxx and 6xxx series aluminium alloys as they are easily weldable when compared to the high strength aluminium alloys such as 2xxx and 7xxx alloys. The main weakness of the fusion welding process (GTA/GMA/EB or LB) is that it consists of an aggregation of constituent precipitation randomly and has cast microstructure. The final microstructure and phase transformation of the welded components depend on the filler material used in the process and also depend on the amount of heat input given during the welding process.

The invention of the solid state joining process known as friction stir welding (FSW) was developed in the year of 1991. The joining of high strength aluminium alloys by this FSW has become much easier and this process has gained a broad application in the aircraft sector for the joining of heat-treatable aluminium alloys. The major advantage in this FSW is that it produces the final product without any distortion. Apart from FSW, the power beam processes such as electron beam (EB) and laser beam (LB) welding have been widely used for welding of high strength and age hardenable Al alloys in the recent years.

In the FSW process, extensive plastic deformation and flow of material assisted by the frictional heat take place at the weld nugget. During the FSW process, high temperature of about 480 °C is obtained in the weld nugget region, in some cases, it has been reported that inchoate melting in the weld nugget occurs due to frictional heat generated during the FSW process. The regions adjoining the weld nugget also get affected by the thermomechanical effects. Thus, the corrosion behavior of the weldment of the Al alloy is expected to alter significantly. The prior/post-weld heat treatment, phase transformations/micro constituents in the weld metal and/or heat affected zone and the residual stresses

that develop during welding may have a vital influence on the SCC behavior. As stated earlier that 6xxx series Al alloys are less susceptible to SCC, FSW 6xxx Al weldments alloys are also less prone to SCC and also SCC of these weldments exhibit better SCC resistance than the parent metal [97]. It is reported that 2219 Al alloy in T87 temper and its friction stir weldment in the as-welded condition are highly resistant to SCC [98]. SCC failures observed in the heat affected zone regions of 7xxx series alloy weldments have been attributed to the degree of sensitization [99].

It is reported that the FSW weldments of moderate strength Al such as 5083, 2219 and 2195 presented better SCC resistance when compared to high strength 7xxx Al alloys, on account of the favorable temper conditions, microstructural features, and corrosion behavior of different regions of the weldment. It is observed that the resistance of the weldments to SCC is influenced by the welding process and technique. In the case of 2195 and 2219 Al alloys, plasma arc welding was found to have a higher susceptibility to SCC than its FSW counterpart [100].

Stress corrosion cracking (SCC) behavior and mechanism of a friction stir welded Al–Zn–Mg–Zr alloy with 0.25% Sc were investigated by DENG et al [101]. It was reported that the thermo-mechanically affected zone on advancing side adjacent to weld nugget zone is the most susceptible to SCC, which can be ascribed to the enrichment of impurity intermetallics, continuously distributed grain boundary precipitates and its stronger galvanic coupling with weld nugget zone from their greater microstructure and micro-chemistry differences.

An electron beam weldment of alloy 7050-T7451 Al-alloy was found to be susceptible to SCC in 3.5% NaCl solution compared to its parent alloy, as assessed by constant load SCC tests at different stress levels. The higher susceptibility was attributed to the considerable level of residual stresses in the EB weldments [102]. HATAMLEH et al [103] produced friction stir welds from 7075 Al alloy in T651 temper and evaluated the SCC behavior of this weldment with and without laser shock peening and shot-peening treatments. The temper condition of the welded plates was modified from T651 to T7351 by artificial aging. The peening treatments were aimed at altering the state of residual stress on the surface in order to improve the SCC behavior. The SSRT data summarized by the authors showed that there was no SCC of the weldments in 3.5% NaCl solution, even in the non-peened condition, which could be attributed to change in temper condition to a more stable/SCC resistant T7351. The limited available information on the SCC behavior of aluminium alloy welds indicates that the alloys welded in the stabilized temper or that were given a post-welding heat treatment may resist the

environmentally induced damage.

SRINIVASAN et al [104] have investigated the SCC behavior of a dissimilar friction stir weldment that comprised 6056 and 7075 Al alloys. In the SSRT tests performed in air and in 3.5% NaCl solution at  $10^{-6} \text{ s}^{-1}$ , the fracture was observed in the TMZ/HAZ region of the 6056 Al alloy, which was the weak region in the joint. Even though numerous pits were observed in the 7075 Al alloy and also in the root region of the weld nugget, there was no SCC. However, when the test was performed at a lower strain rate ( $10^{-7} \text{ s}^{-1}$ ), SCC was noticed in the 7075 parent alloy, revealing the significant influence of strain rate in evaluating SCC of this dissimilar aluminium alloy weldment.

PAGLIA et al [99] studied the effect of short term heat treatment on the friction stir welded 7075-T7451 alloys the short term heat maximum of 280 °C was applied and the SCC resistance increased and the fracture region transferred from HAZ to nugget.

Intergranular corrosion tests following friction stir welding of aluminum alloy 7075-T651 were studied by LUMSDEN et al [105], they have concluded that following FSW of AA 7075-T651, weld zones were susceptible to intergranular attack. The hottest regions within the HAZ were the most susceptible to intergranular corrosion. The weld nugget and deformed region of the TMAZ were also susceptible to intergranular corrosion, but to a lesser extent than the hottest region of the HAZ. The mechanism of intergranular corrosion best correlated to a Cu depletion model linking intergranular corrosion with pitting corrosion.

#### 4 Stress corrosion cracking behavior of 7xxx metal matrix composites

Aluminum metal matrix composites have better mechanical and wear properties as compared to monolithic counterpart. The superior properties can be attributed to the matrix phase reinforced with hard secondary phase in the form of particulates, whiskers or fibers. These reinforcements add their additional properties to matrix phase. But, when coming to the corrosion of metal matrix composites, it is uncertain. Corrosion susceptibility may increase or decrease with the addition of the particles reinforcement and it depends on processing parameters involved in making the MMC as well as on the metal reinforcement combination. The corrosion problems that are likely to occur in metal matrix composites (MMCs) are as follows [106]: 1) Galvanic effects between the matrix and reinforcing phase, 2) Selective corrosion at the matrix/ reinforcement interface, 3) Corrosion caused due to defect during manufacturing of matrix.

MMCs are manufactured with incorporating the ceramic particles or insulating particles such as boron, alumina and silicon carbide etc., little or no galvanic reaction between reinforcement particles and the aluminium matrix would be expected, but, when manufacturing the MMC, a strong interfacial phase is formed which binds the matrix and reinforcement. If this interfacial phase behaves as cathodic or anodic potential then it may favor corrosion to occur. This corrosion leads to pit formation and acts as a crack initiation site, upon loading or application of stress at this site leads to SCC failure. Further aging of this high strength heat treatable Al MMCS has a profound effect on the SCC behavior. Another reason for SCC failures of MMCS is attributed to buildup of a very huge dislocation density due to presence of immiscible reinforcement particles which raises the stress concentration at the interface, and may favor fast dissolution of atoms in the composite compared to metal alloy and also de-bonding between the matrix/interface would support the mechanism of stress concentration at the interface in the stimulation of the corrosion process [107].

SHIMIZU et al [108] studied the corrosion characteristics of Al 6061 based metal matrix composites (MMCs) containing carbon fibers, alumina fibers or silicon carbide whiskers (SiC<sub>w</sub>) and the effects of aging heat treatment on the stress corrosion cracking resistance of SiC<sub>w</sub>-Al 7075 MMC were studied in chloride solutions. They observed that the resistance to pit initiation was the same for both monolithic alloy as well as the SiC<sub>w</sub>-Al 6061 MMC. Upon initiation of pitting further damage will proceed by formation of crevices between the matrix and the reinforcement and by the dissolution of the latter in the pits. While for Al 7075 metal matrix composite, aging at 170 °C for more than 1 h and subsequently aging at 110 °C made MMCs resistance to SCC due to formation of precipitates adjacent to the SiC<sub>w</sub>-Al 7075 interface make them noble.

WINKLER and FLOWER [109] studied the SCC behavior of 7Al-6Zn-1Mg and Al-6Zn-1Mg-1Ag (7xxx) MMCs reinforced with Al<sub>2</sub>O<sub>3</sub> fibers. They reported that Ag has significant role in SCC resistance in MMC. They have observed that MMC containing Ag has higher resistance to SCC as compared to the MMCs without Ag and also stated that the pitting tends to initiate at the fiber/matrix interfaces due to galvanic effect between the Fe-rich particles and Ti-rich at the interface and the matrix. SCC in MMC initiates due to microsegregation of the Mg at the matrix/fiber interface which increases the transportation of hydrogen making the composite brittle. Furthermore, the investigation of fracture surface of MMCs suggests that both the anodic dissolution and hydrogen embrittlement mechanism are engaged in stress corrosion crack initiation and

propagation. Also, the SCC occurs due to microsegregation of Mg at the fiber/matrix region which enhances hydrogen transportation, hence embrittles the composite. Evidence of corrosion-product free cracks observed along grain boundaries in the metal matrix originating from pitting regions strongly suggests that both the dissolution and embrittlement mechanism are involved in stress corrosion crack initiation and propagation of these cast Al–6Zn–1Mg and Al–6Zn–1Mg–1Ag composites.

## 5 Conclusions

1) It has been noticed that stress corrosion cracking is the major drawback in 7xxx aluminum alloy even it possesses high mechanical properties with high specific strength. From past decade, most of the researchers have worked to understand the mechanism of SCC and applied various methods such as altering alloy composition, microstructure, heat treatment, thermo-mechanical treatments and surface treatments to improve the SCC resistance for this alloys.

2) Hydrogen induced cracking and anodic dissolution assisted cracking are the two extensively reported SCC mechanisms in 7xxx Al alloys. Grain size and orientation, precipitation along grain boundary and dislocations influence the SCC behavior of Al alloys. Various novel heat treatment procedures like over aging, retrogression and re-aging and multi-step aging have been developed to improve the SCC resistance of Al alloys. The inhibiting re-crystallization by Sc, Zr, Er and Cr alloying has shown to enhance the SCC resistance of Al alloys.

3) It was observed that SCC susceptibility and strength of this alloy act as a counterpart with each other. Most of the research work was done to balance the SCC susceptibility and strength of the alloy. The low resistance to SCC in 7xxx series weldments is due to the transformation that takes place during welding in the different regions of the weldment and the residual stresses generated during the welding are attributed to the SCC failure.

## References

- [1] GAO J, QUESNEL D J. Enhancement of the stress corrosion sensitivity of AA5083 by heat treatment [J]. *Metallurgical and Materials Transactions A*, 2011, 42: 356–364.
- [2] RICKER RHJARE. Stress-corrosion cracking [M]//*Metals Handbook*. Geauge: ASM International, 1987.
- [3] TURNBULL A, HORNER D, CONNOLLY B. Challenges in modelling the evolution of stress corrosion cracks from pits [J]. *Engineering Fracture Mechanics*, 2009, 76: 633–640.
- [4] PARKINS R. Significance of pits, crevices, and cracks in environment-sensitive crack growth [J]. *Materials Science and Technology*, 1985, 1: 480–486.
- [5] SPEIDEL M O. Stress corrosion cracking of aluminum alloys [J]. *Metallurgical Transactions A*, 1975, 6: 631–651.
- [6] TROIANO A R. The role of hydrogen and other interstitials in the mechanical behavior of metals [J]. *Trans ASM*, 1960, 52: 54–80.
- [7] YOUNG L M. Microstructural dependence of aqueous-environment assisted crack growth and hydrogen uptake in AA7050 [D]. Charlottesville, VA: University of Virginia, 1999.
- [8] ALBRECHT J, THOMPSON A, BERNSTEIN I. The role of microstructure in hydrogen-assisted fracture of 7075 aluminum [J]. *Metallurgical Transactions A*, 1979, 10: 1759–1766.
- [9] TALIANKER M, CINA B. Retrogression and reaging and the role of dislocations in the stress corrosion of 7000-type aluminum alloys [J]. *Metallurgical Transactions A*, 1989, 20: 2087–2092.
- [10] BURLEIGH T. The postulated mechanisms for stress corrosion cracking of aluminum alloys: A review of the literature 1980–1989 [J]. *Corrosion*, 1991, 47: 89–98.
- [11] BOBBY-KANNAN M, RAJA V, RAMAN R, MUKHOPADHYAY A. Influence of multistep aging on the stress corrosion cracking behavior of aluminum alloy 7010 [J]. *Corrosion*, 2003, 59: 881–889.
- [12] SPROWLS D O, BROWN R H. Resistance of wrought high-strength aluminum alloys to stress corrosion [M]. New York: Aluminum Company of America, 1962.
- [13] HAYNIE F H, BOYD W K. Stress-corrosion cracking of aluminum alloys [M]. Battelle Memorial Inst Columbus, OH: Defense Metals Information Center, 1966.
- [14] RINKER J, MAREK M, SANDERS J. Microstructure, toughness and SCC behavior of 2020 [C]//*Second International Aluminum-Lithium Conference*: Monterey, California, 1983.
- [15] VASUDEVAN A, ZIMAN P, JHA S, SANDERS T. Stress corrosion resistance of Al–Cu–Li–Zr alloys [C]//*Aluminium-lithium Alloys III*. London: Institute of Metals, 1986: 303–309.
- [16] HOLROYD N, GRAY A, SCAMANS G, HERMANN R. Environment-sensitive fracture of Al–Li–Cu–Mg alloys [C]//*Aluminium Lithium Alloys III*. London: Institute of Metals, 1985: 310–320.
- [17] BROWN B F. Stress-corrosion cracking in high strength steels and in titanium and aluminum alloys [R]. Washington D C: Naval Research Lab, 1972.
- [18] KNIGHT S, BIRBILIS N, MUDDLE B, TRUEMAN A, LYNCH S. Correlations between intergranular stress corrosion cracking, grain-boundary microchemistry, and grain-boundary electrochemistry for Al–Zn–Mg–Cu alloys [J]. *Corrosion Science*, 2010, 52: 4073–4080.
- [19] ROBSON J, PRANGNELL P. Predicting recrystallised volume fraction in aluminium alloy 7050 hot rolled plate [J]. *Materials Science and Technology*, 2002, 18: 607–614.
- [20] TSAI W, DUH J, YEH J, LEE J, CHANG Y. Effect of pH on stress corrosion cracking of 7050-T7451 aluminum alloy in 3.5wt% NaCl solution [J]. *Corrosion*, 1990, 46: 444–449.
- [21] LIN J C, LIAO H L, JEHNG W D, CHANG C H, LEE S L. Effect of heat treatments on the tensile strength and SCC-resistance of AA7050 in an alkaline saline solution [J]. *Corrosion Science*, 2006, 48: 3139–3156.
- [22] LIAO H L, LIN J C, LEE S L. Effect of pre-immersion on the SCC of heat-treated AA7050 in an alkaline 3.5% NaCl [J]. *Corrosion Science*, 2009, 51: 209–216.
- [23] REDA Y, ABDEL-KARIM R, ELMAHALLAWI I. Improvements in mechanical and stress corrosion cracking properties in Al-alloy 7075 via retrogression and reaging [J]. *Materials Science and Engineering A*, 2008, 485: 468–475.
- [24] GRUHL W. The stress-corrosion behavior of high-strength Al–Zn–Mg alloys [C]//*Aluminium Alloys in the Aircraft Industries 1978*: 171–174.
- [25] GRUHL W. Stress corrosion cracking of high strength aluminum alloys [J]. *Zeitschrift Fuer Metallkunde*, 1984, 75: 819–826.

- [26] SPEIDEL M O, HYATT M V. Stress-corrosion cracking of high-strength aluminum alloys [C]//Advances in Corrosion Science and Technology. New York and London: Springer, 1972: 115–335.
- [27] SARKAR B, MAREK M, STARKE E. The effect of copper content and heat treatment on the stress corrosion characteristics of Al–6Zn–2Mg–xCu alloys [J]. Metallurgical Transactions A, 1981, 12: 1939–1943.
- [28] BIRNBAUM H K. Mechanisms of hydrogen related fracture of metals [R]. Washington D C: Naval Research Lab, 1989.
- [29] SONG R, TSENG M, ZHANG B, LIU J, JIN Z, SHIN K. Grain boundary segregation and hydrogen-induced fracture in 7050 aluminium alloy [J]. Acta Materialia, 1996, 44: 3241–3248.
- [30] XU D, BIRBILIS N, ROMETSCH P. Effect of S-phase dissolution on the corrosion and stress corrosion cracking of an as-rolled Al–Zn–Mg–Cu alloy [J]. Corrosion, The Journal of Science and Engineering, 2012, 68: 035001.
- [31] WU X Z, XIAO D H, ZHU Z M, LI X X, CHEN K H. Effects of Cu/Mg ratio on microstructure and properties of AA7085 alloys [J]. Transactions of Nonferrous Metals Society of China, 2014, 24: 2054–2060.
- [32] KNIGHT S, POHL K, HOLROYD N, BIRBILIS N, ROMETSCH P, MUDDLE B, GOSWAMI R, LYNCH S P. Some effects of alloy composition on stress corrosion cracking in Al–Zn–Mg–Cu alloys [J]. Corrosion Science, 2015, 98: 50–62.
- [33] SCAMANS G M, ALANI R, SWANN P R. Pre-exposure embrittlement and stress corrosion failure in Al Zn Mg alloys [J]. Corrosion Science, 1976, 16: 443–459.
- [34] CHEN K, FANG H C, ZHANG Z, CHEN X, LIU G. Effect of Yb, Cr and Zr additions on recrystallization and corrosion resistance of Al–Zn–Mg–Cu alloys [J]. Materials Science and Engineering A, 2008, 497: 426–431.
- [35] LI Z, XIONG B, ZHANG Y, ZHU B, WANG F, LIU H. Ageing behavior of an Al–Zn–Mg–Cu alloy pre-stretched thick plate [J]. Journal of University of Science and Technology Beijing: Mineral, Metallurgy, Material, 2007, 14: 246–250.
- [36] LIU Ying-ying, XIA Chang-qing, PENG Xiao-min. Effect of heat treatment on microstructures and mechanical properties of Al–6Zn–2Mg–1.5Cu–0.4Er alloy [J]. Journal of Central South University, 2010, 17: 24–27.
- [37] DENG Y, YIN Z, ZHAO K, DUAN J, HU J, HE Z. Effects of Sc and Zr microalloying additions and aging time at 120 C on the corrosion behaviour of an Al–Zn–Mg alloy [J]. Corrosion Science, 2012, 65: 288–298.
- [38] FANG H, CHAO H, CHEN K. Effect of Zr, Er and Cr additions on microstructures and properties of Al–Zn–Mg–Cu alloys [J]. Materials Science and Engineering A, 2014, 610: 10–16.
- [39] AU H. Pitting and crack initiation in high strength aluminum alloys for aircraft applications [J]. Massachusetts Institute of Technology, 1996.
- [40] HANDBOOK A. Aluminum and aluminum alloys [M]. Geauge: ASM International, 1993.
- [41] MURRAY G, LAMB H, GODARD H. Role of iron in aluminium on the initiation of pitting in water [J]. British Corrosion Journal, 1967, 2: 216–218.
- [42] HUAN S, WEI C, DA S, JUN W, SUN B D. Effects of silicon content on microstructure and stress corrosion cracking resistance of 7050 aluminum alloy [J]. Transactions of Nonferrous Metals Society of China, 2014, 24: 2307–2313.
- [43] HOLROYD N. Environment-induced cracking of high-strength aluminum alloys [C]//Environment-Induced Cracking of Metals, Houston, TX: NACE International, 1990: 311.
- [44] SONG R, DIETZEL W, ZHANG B, LIU W, TSENG M, ATRENS A. Stress corrosion cracking and hydrogen embrittlement of an Al–Zn–Mg–Cu alloy [J]. Acta Materialia, 2004, 52: 4727–4743.
- [45] SONG M, CHEN K. Effects of the enhanced heat treatment on the mechanical properties and stress corrosion behavior of an Al–Zn–Mg alloy [J]. Journal of Materials Science, 2008, 43: 5265–5273.
- [46] GAO M, FENG C, WEI R P. An analytical electron microscopy study of constituent particles in commercial 7075-T6 and 2024-T3 alloys [J]. Metallurgical and Materials Transactions A, 1998, 29: 1145–1151.
- [47] BUHA J, LUMLEY R, CROSKY A. Secondary ageing in an aluminium alloy 7050 [J]. Materials Science and Engineering A, 2008, 492: 1–10.
- [48] de ARDO A, TOWNSEND R. The effect of microstructure on the stress-corrosion susceptibility of a high purity Al–Zn–Mg alloy in a NaCl solution [J]. Metallurgical Transactions, 1970, 1: 2573–2581.
- [49] PUIGGALI M, ZIELINSKI A, OLIVE J, RENAULD E, DESJARDINS D, CID M. Effect of microstructure on stress corrosion cracking of an Al–Zn–Mg–Cu alloy [J]. Corrosion Science, 1998, 40: 805–819.
- [50] SUN X, ZHANG B, LIN H, ZHOU Y, SUN L, WANG J, et al. Correlations between stress corrosion cracking susceptibility and grain boundary microstructures for an Al–Zn–Mg alloy [J]. Corrosion Science, 2013, 77: 103–112.
- [51] VASUDEVAN A K, DOHERTY R. Grain boundary ductile fracture in precipitation hardened aluminum alloys [J]. Acta Metallurgica, 1987, 35: 1193–1219.
- [52] MCEVILY A, CLARK J, BOND A. Effect of thermal-mechanical processing on the fatigue and stress-corrosion properties of an Al–Sn–Mg alloy [J]. ASM Trans Quart, 1967, 60: 661–671.
- [53] TAYLOR I, EDGAR R. A study of stress-corrosion in Al–Zn–Mg alloys [J]. Metallurgical Transactions, 1971, 2: 833–839.
- [54] THOMAS G, NUTTING J. Electron microscope studies of alloys based on the aluminum-zinc-magnesium system [J]. J Inst Metals, 1959, 88: 1960.
- [55] TANAKA M, DIF R, WARNER T. Chemical composition profiles across grain boundaries in T6, T79 and T76 tempered AA7449 alloy [J]. Materials Science Forum, 2002, 369–402: 1449–1454.
- [56] TSAI T, CHUANG T. Role of grain size on the stress corrosion cracking of 7475 aluminum alloys [J]. Materials Science and Engineering A, 1997, 225: 135–144.
- [57] TSAI T, CHUANG T. Atmospheric stress corrosion cracking of a superplastic 7475 aluminum alloy [J]. Metallurgical and Materials Transactions A, 1996, 27: 2617–2627.
- [58] CINA B. Reducing the susceptibility of alloys, particularly aluminium alloys, to stress corrosion cracking: U.S. Patent 3856584 [P]. 1974–12–24.
- [59] PARK J. Influence of retrogression and reaging treatments on the strength and stress corrosion resistance of aluminium alloy 7075-T6 [J]. Materials Science and Engineering A, 1988, 103: 223–231.
- [60] VIANA F, PINTO A, SANTOS H, LOPES A. Retrogression and re-ageing of 7075 aluminium alloy: microstructural characterization [J]. Journal of Materials Processing Technology, 1999, 92: 54–59.
- [61] XU D, BIRBILIS N, ROMETSCH P. The effect of pre-ageing temperature and retrogression heating rate on the strength and corrosion behaviour of AA7150 [J]. Corrosion Science, 2012, 54: 17–25.
- [62] ROBINSON J, WHELAN S, CUDD R. Retrogression and re-aging of 7010 open die forgings [J]. Materials Science and Technology, 1999, 15: 717–724.
- [63] BAYDOGAN M, CIMENOGLU H, KAYALI E S, RASTY J. Improved resistance to stress-corrosion-cracking failures via optimized retrogression and reaging of 7075-T6 aluminum sheets [J]. Metallurgical and Materials Transactions A, 2008, 39: 2470–2476.
- [64] LI W B, PAN Q L, XIAO Y P, HE Y B, LIU X Y. Microstructure and



- mechanical properties of Al–Zn–Cu–Mg–Sc–Zr alloy after retrogression and re-aging treatments [J]. *Journal of Central South University of Technology*, 2011, 18: 279–284.
- [65] RAJAN K, WALLACE W, BEDDOES J. Microstructural study of a high-strength stress-corrosion resistant 7075 aluminium alloy [J]. *Journal of Materials Science*, 1982, 17: 2817–2824.
- [66] FERRER C, KOUL M, CONNOLLY B, MORAN A. Improvements in strength and stress corrosion cracking properties in aluminum alloy 7075 via low-temperature retrogression and re-aging heat treatments [J]. *Corrosion*, 2003, 59: 520–528.
- [67] OLIVEIRA A, de BARROS M, CARDOSO K, TRAVESSA D. The effect of RRA on the strength and SCC resistance on AA7050 and AA7150 aluminium alloys [J]. *Materials Science and Engineering A*, 2004, 379: 321–326.
- [68] SHASTRY C, LEVY M, JOSHI A. The effect of solution treatment temperature on stress corrosion susceptibility of 7075 aluminium alloy [J]. *Corrosion Science*, 1981, 21: 673–688.
- [69] JOSHI A, SHASTRY C, LEVY M. Effect of heat treatment on solute concentration at grain boundaries in 7075 aluminum alloy [J]. *Metallurgical Transactions A*, 1981, 12: 1081–1088.
- [70] LI J F, PENG Z W, LI C X, JIA Z Q, CHEN W J, ZHENG Z Q. Mechanical properties, corrosion behaviors and microstructures of 7075 aluminium alloy with various aging treatments [J]. *Transactions of Nonferrous Metals Society of China*, 2008, 18: 755–762.
- [71] SILVA G, RIVOLTA B, GEROSA R, DERUDI U. Study of the SCC behavior of 7075 aluminum alloy after one-step aging at 163 °C [J]. *Journal of Materials Engineering and Performance*, 2013, 22: 210–214.
- [72] OU B L, YANG J G, WEI M Y. Effect of homogenization and aging treatment on mechanical properties and stress-corrosion cracking of 7050 alloys [J]. *Metallurgical and Materials Transactions A*, 2007, 38: 1760–1773.
- [73] MAGNIN T. Recent advances in the environment sensitive fracture mechanisms of aluminium alloys [J]. *Materials Science Forum: Trans Tech Publ*, 1996, 217: 83–94.
- [74] TIEN J K, NAIR S V, JENSEN R R. Dislocation sweeping of hydrogen and hydrogen embrittlement [C]//*Hydrogen Effects in Metals NY: Metallurgical Society of AIME*, 1981: 37–56.
- [75] TAHERI M, ALBRECHT J, BERNSTEIN I, THOMPSON A. Strain-rate effects on hydrogen embrittlement of 7075 aluminum [J]. *Scripta Metallurgica*, 1979, 13: 871–875.
- [76] HOEPPNER D W, ARRISCORRETA C A. Exfoliation corrosion and pitting corrosion and their role in fatigue predictive modeling: State-of-the-art review [J]. *International Journal of Aerospace Engineering*, 2012: 191879.
- [77] BRAUN R. Slow strain rate testing of aluminum alloy 7050 in different tempers using various synthetic environments [J]. *Corrosion*, 1997, 53: 467–474.
- [78] BOCKRIS J O M, REDDY A K. *Modern electrochemistry: An introduction to an interdisciplinary area* [M]. Berlin: Springer Science & Business Media, 2012.
- [79] PENTLAND N, BOCKRIS J M, SHELDON E. Hydrogen evolution reaction on copper, gold, molybdenum, palladium, rhodium, and iron mechanism and measurement technique under high purity conditions [J]. *Journal of the Electrochemical Society*, 1957, 104: 182–194.
- [80] MUELLER M, THOMPSON A, BERNSTEIN I. Stress corrosion behavior of 7075 aluminum in 1N aluminum chloride solutions [J]. *Corrosion*, 1985, 41: 127–136.
- [81] ONORO J, RANNINGER C. Stress-corrosion-cracking behavior of heat-treated Al–Zn–Mg–Cu alloy with temperature [J]. *Materials Science*, 1999, 35: 509–514.
- [82] KANNAN M B, RAJA V, MUKHOPADHYAY A. Determination of true stress corrosion cracking susceptibility index of a high strength Al alloy using glycerin as the non-corrosive atmosphere [J]. *Scripta Materialia*, 2004, 51: 1075–1079.
- [83] ROUT P K, GHOSH M, GHOSH K. Effect of solution pH on electrochemical and stress corrosion cracking behaviour of a 7150 Al–Zn–Mg–Cu alloy [J]. *Materials Science and Engineering A*, 2014, 604: 156–165.
- [84] TROMANS D, PATHANIA R. *The electrochemical society. Extended Abstracts* [R]. Pennington, New Jersey: The Electrochemical Society, 1969.
- [85] DESCHAMPS A, LIVET F, BRECHET Y. Influence of predeformation on ageing in an Al–Zn–Mg alloy—I. Microstructure evolution and mechanical properties [J]. *Acta Materialia*, 1998, 47: 281–292.
- [86] FOOLADFAR H, HASHEMI B, YOUNESI M. The effect of the surface treating and high-temperature aging on the strength and SCC susceptibility of 7075 aluminum alloy [J]. *Journal of Materials Engineering and Performance*, 2010, 19: 852–859.
- [87] WATERLOO G, HANSEN V, GJØNNES J, SKJERVOLD S. Effect of predeformation and preaging at room temperature in Al–Zn–Mg–(Cu, Zr) alloys [J]. *Materials Science and Engineering A*, 2001, 303: 226–233.
- [88] WANG D, NI D, MA Z. Effect of pre-strain and two-step aging on microstructure and stress corrosion cracking of 7050 alloy [J]. *Materials Science and Engineering A*, 2008, 494: 360–366.
- [89] WANG D, MA Z, GAO Z. Effects of severe cold rolling on tensile properties and stress corrosion cracking of 7050 aluminum alloy [J]. *Materials Chemistry and Physics*, 2009, 117: 228–233.
- [90] NGUYEN D, THOMPSON A, BERNSTEIN I. Microstructural effects on hydrogen embrittlement in a high purity 7075 aluminum alloy [J]. *Acta Metallurgica*, 1987, 35: 2417–2425.
- [91] YUE T, DONG C, YAN L, MAN H. The effect of laser surface treatment on stress corrosion cracking behaviour of 7075 aluminium alloy [J]. *Materials Letters*, 2004, 58: 630–635.
- [92] CHAN C, YUE T, MAN H. The effect of excimer laser surface treatment on the pitting corrosion fatigue behaviour of aluminium alloy 7075 [J]. *Journal of Materials Science*, 2003, 38: 2689–2702.
- [93] YUE T, YAN L, DONG C, CHAN C. Stress corrosion cracking behaviour of laser treated aluminium alloy 7075 using a slow strain rate test [J]. *Materials Science and Technology*, 2005, 21: 961–966.
- [94] YUE T, YAN L, CHAN C. Stress corrosion cracking behavior of Nd: YAG laser-treated aluminum alloy 7075 [J]. *Applied Surface Science*, 2006, 252: 5026–5034.
- [95] VENUGOPAL A, PANDA R, MANWATKAR S, SREEKUMAR K, KRISHNA L R, SUNDARARAJAN G. Effect of micro arc oxidation treatment on localized corrosion behaviour of AA7075 aluminum alloy in 3.5% NaCl solution [J]. *Transactions of Nonferrous Metals Society of China*, 2012, 22: 700–710.
- [96] VENUGOPAL A, PANDA R, MANWATKAR S, SREEKUMAR K, RAMAKRISHNA L, SUNDARARAJAN G. Effect of microstructure on the localized corrosion and stress corrosion behaviours of plasma-electrolytic-oxidation-treated AA7075 aluminum alloy forging in 3.5 wt.% NaCl solution [J]. *International Journal of Corrosion*, 2012: 823967.
- [97] LIM S, KIM S, LEE C G, KIM S. Stress corrosion cracking behavior of friction-stir-welded Al 6061-T651 [J]. *Metallurgical and Materials Transactions A*, 2005, 36: 1977–1980.
- [98] SUREKHA K, MURTY B, RAO K P. Microstructural characterization and corrosion behavior of multipass friction stir processed AA2219 aluminium alloy [J]. *Surface and Coatings Technology*, 2008, 202: 4057–4068.
- [99] PAGLIA C, CARROLL M, PITTS B, REYNOLDS T, BUCHHEIT R. Strength, corrosion and environmentally assisted cracking of a 7075-T6 friction stir weld [J]. *Materials Science Forum*, 2002, 396–402: 1677–1684.

- [100] HU W, MELETIS E I. Corrosion and environment-assisted cracking behavior of friction stir welded Al 2195 and Al 2219 alloys [J]. Materials Science Forum: Trans Tech Publ, 2000, 331: 1683–1688.
- [101] DENG Y, PENG B, XU G, PAN Q, YE R, WANG Y, et al. Stress corrosion cracking of a high-strength friction-stir-welded joint of an Al–Zn–Mg–Zr alloy containing 0.25 wt.% Sc [J]. Corrosion Science, 2015, 100: 57–72.
- [102] CIOMPI E, LANCIOTTI A. Susceptibility of 7050-T7451 electron beam welded specimens to stress corrosion [J]. Engineering Fracture Mechanics, 1999, 62: 463–476.
- [103] HATAMLEH O, SINGH P M, GARMESTANI H. Corrosion susceptibility of peened friction stir welded 7075 aluminum alloy joints [J]. Corrosion Science, 2009, 51: 135–143.
- [104] SRINIVASAN P B, DIETZEL W, ZETTLER R, DOS SANTOS J, SIVAN V. Stress corrosion cracking susceptibility of friction stir welded AA7075–AA6056 dissimilar joint [J]. Materials Science and Engineering A, 2005, 392: 292–300.
- [105] LUMSDEN J, MAHONEY M, POLLOCK G, RHODES C. Intergranular corrosion following friction stir welding of aluminum alloy 7075-T651 [J]. Corrosion, 1999, 55: 1127–1135.
- [106] LUCAS K A, CLARKE H. Corrosion of aluminium-based metal matrix composites [M]. Taunton: Research Studies Press/Chichester: John Wiley, 1993.
- [107] MONTICELLI C, ZUCCHI F, BRUNORO G, TRABANELLI G. Stress corrosion cracking behaviour of some aluminium-based metal matrix composites [J]. Corrosion Science, 1997, 39: 1949–1963.
- [108] SHIMIZU Y, NISHIMURA T, MATSUSHIMA I. Corrosion resistance of Al-based metal matrix composites [J]. Materials Science and Engineering A, 1995, 198: 113–138.
- [109] WINKLER S, FLOWER H. Stress corrosion cracking of cast 7xxx aluminium fibre reinforced composites [J]. Corrosion Science, 2004, 46: 903–915.

## 7xxx 铝合金的应力腐蚀行为综述

A. C. UMAMAHESHWER RAO<sup>1</sup>, V. VASU<sup>1</sup>, M. GOVINDARAJU<sup>2</sup>, K. V. SAI SRINADH<sup>1</sup>

1. Department of Mechanical Engineering, National Institute of Technology Warangal, Warangal 506004, India;

2. Nonferrous Materials Technology Development Centre, Hyderabad-500 058, 500005, India

**摘 要:** 应力腐蚀是材料在应力和腐蚀环境双重作用下使材料力学性能下降的行为。对于八种系列铝合金, 2xxx、5xxx、7xxx 铝合金对于应力腐蚀敏感。由于其优越的力学性能, 7xxx 铝合金广泛应用于航空、军事和结构工业。在这些 7xxx 铝合金中, 应力腐蚀严重影响其力学性能, 使其在服役过程中发生灾难性的失效。因此, 研究该合金的应力腐蚀行为具有重要意义。本文综述了合金成分对合金在不同热处理条件下的显微组织演变, 还综述了改善 7xxx 合金应力腐蚀性能的形变热处理和表面改性方法。此外, 还综述了应力、预应变、合金成分和腐蚀环境对应力腐蚀行为的影响。还综述了焊缝、7xxx 金属基复合材料和激光表面处理合金的应力腐蚀行为。

**关键词:** 7xxx 铝合金; 应力腐蚀; 热处理; 显微组织; 腐蚀环境; 形变热处理

(Edited by Yun-bin HE)